INCORPORATING TWO-DIMENSIONAL, INORGANIC, EXTENDED-LATTICE STRUCTURES AND MAGNETIC PROPERTIES INTO ULTRATHIN ORGANIC FILMS

By

CANDACE TRICIA SEIP

A DISSERTATION PRESENTED TO THE GRADUATE SCHOOL
OF THE UNIVERSITY OF FLORIDA IN PARTIAL FULFILLMENT
OF THE REQUIREMENTS FOR THE DEGREE OF
DOCTOR OF PHILOSOPHY

UNIVERSITY OF FLORIDA

1997

To Mom and Dad

&

My Grandparents.

ACKNOWLEDGMENTS

I would like to thank my advisor Dr. Daniel Talham for letting me work with him during my time in Florida. He has taught me many skills that I am sure to take with me wherever I go. I am also grateful to Dr. Mark Meisel for performing all the static magnetic measurements on each manganese-containing LB film. I would also like to thank him for all his useful discussions pertaining to magnetism. I also thank the University of Florida Major Analytical Instrumentation Center for the use of their X-ray photoelectron spectrometer and electron microscope, and especially Eric Lambers for many helpful XPS discussions and Augusto Morrone for providing instruction on the operation of the electron microscope. Special thanks go to Andy Boeckl for performing X-ray diffraction measurements on all the LB films. I also would like to thank my Ph.D. committee members Dr. Russell Drago, Dr. Dave Richardson, Dr. John Reynolds, and Dr. Elizabeth Seiberling, for their dedication in attending my seminars and oral examination and their insightful comments and questions, which have proven to be very useful in helping me attain a greater knowledge and understanding of my research.

I am indebted to all my undergraduate chemistry professors, especially Dr. Lynn Mihichuk and Dr. Keith Johnson. They provided me with a solid understanding of chemistry, introduced me to research, and encouraged me to further my education in chemistry.

I would like to thank my parents, Ken and Gayle Seip, for all their love, constant encouragement and support. They provided me with the confidence to believe in myself and made everything I've accomplished, possible. Special thanks go to my Uncle David and Aunt Julie for lending me their laptop computer, which helped immensely in the preparation of this dissertation.

Finally, I would like to acknowledge some of my friends for their companionship and support. I thank Angela for being an especially good friend and a person I can always count on. I thank her for being a great shopping buddy and for occasionally reminding me that I can't spend all my time in the lab! I also thank her for initiating me into the Energizer skating club, which provided me with hours, and miles, of endless fun with only minor injuries. I thank "Bry Guy" for being a special friend who was always there whenever I needed him. I hope you have fun while you're away, and hope you don't get sea sick! I would also like to thank Steve Joerg for his special friendship, chemistry discussions, and spiritual support throughout the years. I also thank my most recent friends, Mary and BJ, for making my last two semesters here a lot of fun. It's too bad you didn't get here sooner! Lastly, I thank Cheryl, Richard, and Treena for being my dear friends for many years. I look forward to the friendship we'll share for many more years to come.

TABLE OF CONTENTS

Page

LIST OF TABLES

LIST OF FIGURES

Abstract of Dissertation Presented to the Graduate School
of the University of Florida in Partial Fulfillment of the
Requirements for the Degree of Doctor of Philosophy

INCORPORATING TWO-DIMENSIONAL, INORGANIC, EXTENDED-LATTICE STRUCTURES AND MAGNETIC PROPERTIES INTO ULTRATHIN ORGANIC FILMS

By

Candace Tricia Seip

May, 1997

Chairman: Daniel R. Talham
Major Department: Chemistry

This dissertation presents experimental results from the fabrication, structural determination, and magnetic characterizations of a series of single layer and multilayer, extended-lattice, divalent metal alkylphosphonate Langmuir-Blodgett (LB) films. LB films of $M(O_3PC_{18}H_{37})\cdot H_2O$, M = Mn, Cd, Co, Mg and $Ca(HO_3PC_{18}H_{37})_2$ were prepared and structurally characterized. The results demonstrate that inorganic extended-lattice networks can be incorporated into ultrathin organic films using LB methodology. Structural identification of single layer and multilayered metal octadecylphosphonate LB films indicate that the organic groups form close-packed, organized films with the metal ions providing extra rigidity and structural order to the films. Metal cations and phosphonate anions comprising the inorganic portions of the LB films occur in ratios equivalent to those observed in analogous metal alkylphosphonate solid-state layered compounds.

Magnetic investigations involving LB films of manganese octadecylphosphonate, $Mn(O_3PC_{18}H_{37})\cdot H_2O$ reveal that the manganese ions undergo two-dimensional

antiferromagnetic Heisenberg exchange at high temperatures. Below 13 K, the LB films undergo a transition to spontaneous long range magnetic order. The manganese spins of the coupled nearest neighbor moments do not exactly cancel due to low site symmetry and weak ferromagnetism is observed below the ordering temperature. In the ordered state, the LB films also exhibit magnetic hysteresis, a signature of magnetic memory. The results demonstrate the first example of a magnetic Langmuir-Blodgett film.

Magnetic susceptibility measurements performed on diluted manganese octadecylphosphonate LB films, $Mn_xCd_{1-x}(O_3PC_{18}H_{37})\cdot H_2O$ exhibit spontaneous magnetization at lower temperatures than those observed in the pure manganese films. The results have been fit to low-dimensional magnetic models. The compiled data presented in this dissertation indicate that magnetic properties usually observed exclusively in inorganic solid-state materials may be incorporated into organic Langmuir-Blodgett films.

CHAPTER 1
INVESTIGATIONS OF TWO-DIMENSIONAL INORGANIC MATERIALS AND INTRODUCTION TO THE LANGMUIR-BLODGETT METHOD

Low Dimensional Inorganic Solids

Low dimensional materials are defined as infinite in one or two spatial directions.[1] Isolated single chains, layers, fibers and thin films of varying but finite thickness all comprise this category. A vast amount of physical phenomena are inherent in systems having restricted dimensionality and are frequently studied to enhance understanding of fundamental theories. As a consequence of the realized properties present in low-dimensional solids, many of these materials have proven to be useful in many technological applications. The investigation of low-dimensional solids and their properties has lead to the discovery of 1-d and 2-d conductors and superconductors, 2-d semiconductor interfaces and 1-d and 2-d molecular crystals and liquid crystals to mention just a few.[1-3]

Many of the physical properties mentioned above are found in inorganic materials, although recently many examples of low-dimensional organic materials having magnetic and electrical properties are emerging.[3] A classic example of a one-dimensional linear chain compound is $K_2Pt(CN)_4Cl_{0.3}3H_2O$, commonly refered to as KCP. The crystal structure of KCP, shown in Figure 1-1,[2] consists of chains of mixed valence platinum ions contained in square planar $Pt(CN)_4$ stacks. Potassium ions fill the channels between the stacks and separate successive platinum chains. The extra chloride ions, also contained in the channels cause the partial oxidation and therefore short bond lengths of the platinum ions. Interest in KCP is mainly attributed to the conductivity that exists along the platinum chains and its overall behavior as a metal.[2] Many other one-dimensional chain

Figure 1-1. The crystal structure of KCP, $K_2Pt(CN)_4Cl_{0.3}3H_2O$. KCP consists of closely spaced square planar $Pt(CN)_4$ groups. Along the platinum chains, KCP is an electrical conductor and behaves as a metal, however, ordinary ionic properties are observed perpendicular to the chains. Potassium cations (dotted circles) and chloride anions (filled circles) are contained in the channels between the platinum stacks and separate the chains of $Pt(CN)_4$ anions. Adapted from reference 2.

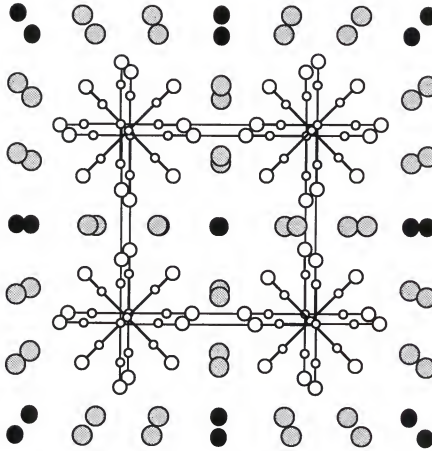

compounds,[4] both organic and inorganic, exist but will not be discussed further in this dissertation. Rather, the focus of this work will concentrate on the two-dimensional materials and their inherent properties, especially those related to magnetism.

After theories of low-dimensional magnetism were established, thorough magnetic investigations of two-dimensional materials began. Initial studies focused mainly on purely inorganic compounds crystallizing in the K_2NiF_4 structure. The K_2NiF_4 structure, as illustrated in Figure 1-2, contains magnetic NiF_2 layers separated by two sheets of nonmagnetic KF.[5] Nearest neighbor magnetic ions within a NiF_2 layer undergo large antiferromagnetic exchange. Interlayer interactions between layers also occur but the order of coupling is much smaller than the intralayer coupling. It was soon realized that any

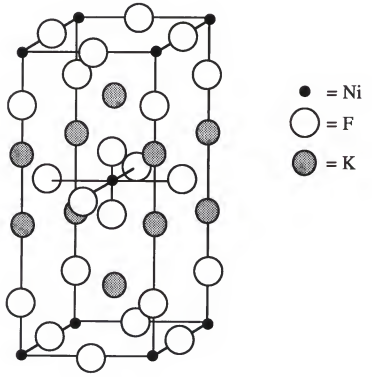

Figure 1-2. Illustration of the unit cell of the K_2NiF_4 structure. Substantial experimental work has been performed on compounds having the K_2NiF_4 structure due to the two-dimensional framework of the metal ions.

deviation from the ideal isotropic two-dimensional system, such as the presence of interlayer coupling, single-ion anisotropy, anisotropy in the exchange mechanism, and crystal imperfections may introduce long-range order at finite temperatures.[6] With this discovery came the need for solid-state materials with more two-dimensional structures.

Organic/Inorganic Layered Compounds

Layered compounds consisting of two-dimensional arrays of inorganic material separated by non-functional organic material are excellent models of two-dimensional systems and are a better approach to reaching two-dimensionality over the classical purely inorganic materials. In these solid-state materials, interactions in the inorganic layers are better confined within each layer since the organic groups force the inorganic layers farther apart. Communication between succesive inorganic layers is dependent upon the size of the organic spacer. As the organic groups become larger, inorganic interlayer interactions diminish. Two classes of solid-state compounds synonymous with two-dimensional models are the alkylammonium metal tetrahalide perovskites and the metal organophosphonates.

In the perovskite familiy, $(C_nH_{2n+1}NH_3)_2MX_4$, where M = a divalent metal ion; X = a halide, metal ions are linked into two-dimensional sheets by sharing equatorial halides with neighboring MX_6 octahedra, as illustrated schematically in Figure 1-3[7]. NH_3^+ groups occupy octahedral holes and are electrostatically held into place by hydrogen bonds between the hydrogens and the halides. Hydrocarbon chains on the ammonium groups are directed away from the metal sheets and therefore separate successive metal layers. The layered nature of the perovskites is clearly shown in the crystal structure of $(C_{10}H_{21}NH_3)_2CdCl_4$,[7] Figure 1-4. In this solid-state material, cadmium ions form two-dimensional layers suspended between layers of alkylammonium groups. Van der Waals interactions between the terminal methyls of the alkylammonium groups of adjacent layers are responsible for keeping consecutive layers together.[7,8]

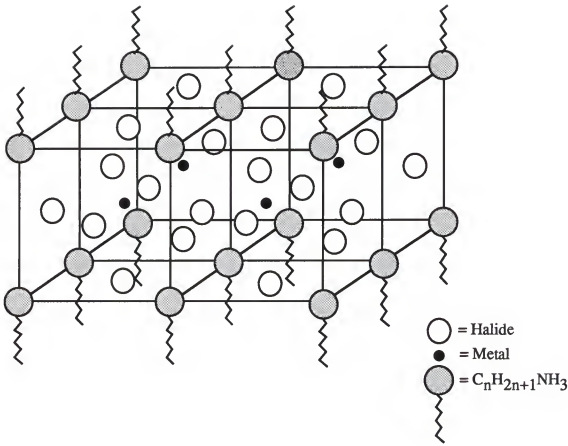

Figure 1-3. Atomic positions of the atoms in alkylammonium metal tetrahalides. The metal ions are linked into a two-dimensional sheet by edge sharing MX_6 octahedra. Nitrogen atoms fit into octahedral holes and the hydrocarbon groups are directed away from the metal ion plane.

Historically, the perovskites have been investigated for three main reasons.[9] The first reason was due to the temperature dependent structural phase transitions that many of the layer perovskite halide salts undergo. With increases in temperature the NH_3^+ groups have free rotation, and the hydrogen bonding that exists between the hydrogens on the NH_3^+ groups and the halides is found to vary.[9] Changes in the color observed in copper

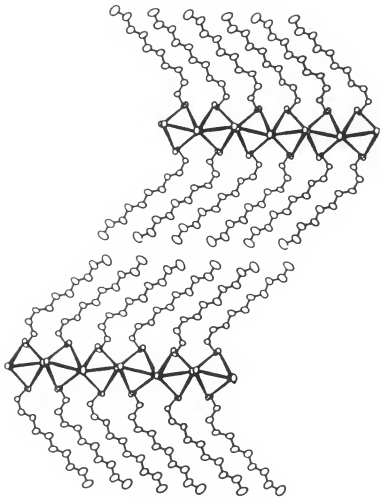

Figure 1-4. Crystal structure of $(C_{10}H_{21}NH_3)_2CdCl_4$.[7] These layer type perovskites have proven to be useful in the study of solid-state two-dimensional compounds.

perovskites as a function of temperature were attributed to these structural transitions.[7] Changes in the structures of the perovskites were also related to interesting lattice vibrations and dielectric properties.[7] Perovskites have also received attention due to the possibility of using the inorganic layers as templates for organic reactions such as polymerization.[9] In metal perovskites possessing organic groups with chemical functionality, the inorganic metal ions direct the organic groups and hold them in place such that they could react with each other stereospecifically to form ordered polymers. In addition to this concept, research on molecular composities has been initiated. The perovskites may be modified in such a way that the properties of the organic groups and inorganic ions complement each other in order to produce a wide variety of new properties. The third major reason that the perovskite halide salts have been of interest involves their interesting magnetic properties. Since these solids model two-dimensional materials, perovskites bearing paramagnetic metal ions have been the focus of low-dimensional magnetic studies in order to probe the theoretical predictions of 2-d magnetism. It is reported that perovskites, $(C_nH_{2n+1}NH_3)_2MCl_4$, with M = Cu and Cr are ferromagnetic[10,11] and those containing Mn are antiferromagnetic.[12] The transition to a magnetically ordered state was in most cases attributed to a crossover from two-dimensionality to three dimensionality since the perovskites are part of a three-dimensional framework.

The transition metal phosphonates, represented by the molecular formula, $M(O_3PC_nH_{2n+1})\cdot H_2O$ where M is a divalent metal ion, are also examples of mixed organic/inorganic layered solids and have been used as low-dimensional model compounds.[9] In these materials, metal ions are bridged by phosphonate groups forming two-dimensional extended-lattice sheets of metal ions separated by the organic substituents on the phosphonate ligands.[13-18] The structure of calcium methylphosphonate is shown in Figure 1-5.[13] Many other divalent metal ions also form complexes with a variety of organophosphonate groups and are structurally similar to calcium methylphosphonate.[14,15,19] In cadmium, manganese, cobalt, zinc, nickel, chromium,

Figure 1-5. Crystal structure of $Ca(O_3PCH_3)\cdot H_2O$. Structural parameters were taken from reference 13. In the metal alkylphosphonates metal ions form two-dimensional sheets suspended between alkylphosphonate groups. Adjacent layers are held together by weak van der Waals interactions between terminal methyl groups on the alkylphosphonates. (Key: Ca - cross-hatched circles; O - small open circles; P - dotted circles; C - shaded circles; H - small shaded circles).

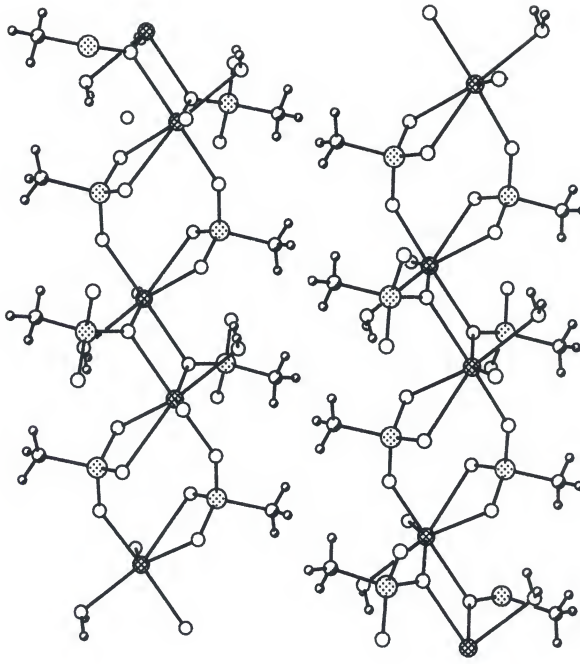

magnesium and some calcium alkylphosphonates, the metal ions are octahedrally coordinated, bonded to six oxygen atoms. Five oxygens are from phosphonate groups and the sixth coordination site is filled by a water molecule. Layers are held together by van der Waals interactions between terminal methyl groups.[13-15,18,20] Divalent metal phosphonates have also shown promise in practical applications in the area of separations, catalysis, chemical sensors, and biological recognition.[21-23] In the solid-state, phosphonate chemistry is rich and continues to be pursued.

Ultrathin Organic Films

The quasi-two-dimensional nature of the previously mentioned layered solids has been useful in investigating phenomena in two-dimensions. However, thin films of these layered materials are possibly more useful in application devices and synthetically, offer more structural control. Two approaches used to achieve organized assemblies of organic molecules at solid surfaces are Langmuir-Blodgett film methods and organic self-assembly methods. Self-assembly procedures have been developed to form single layers and multilayers of tetravalent Zr[24-29] and Hf[30] and divalent Zn and Cu[23] organophosphonates for potential applications ranging from non-linear optics[28,29] and separations[23] to chemical sensors[23] and interfaces.[24] Problems related to most self-assembled films is their fragility and lack of long range structural order.[30] Researchers also recognize the potential of Langmuir-Blodgett films in a variety of industrial applications such as molecular electronics, microelectronics, optics, biosensors, and catalysis,[31-33] to more academic applications such as cell membrane models and two-dimensional model compounds.[34,35] Thin films having a layered nature are excellent models for probing chemistry and physics restricted to two-dimensions. Organic/Inorganic alternating layered Langmuir-Blodgett films are especially useful in this area. They may readily be engineered to maximize the distance between the inorganic lattices by systematically increasing the size of the organic groups between the inorganic layers.

This dissertation focuses on research based on Langmuir-Blodgett films of a variety of divalent metal alkylphosphonates. The reason for choosing phosphonate molecules in conjunction with the LB method of synthesis is dual. First, the LB technique offers much control over the interlayer spacings between inorganic ions. Secondly, phosphonic acid containing a long hydrocarbon chain was the chosen amphiphile since in the solid-state, single crystals of the metal phosphonates containing small organic groups are difficult to synthesize and are almost impossible to obtain in crystalline form when the phosphonates contain alkyl groups consisting of more than six carbon atoms. To date, no single crystal X-ray diffraction data have been reported on any divalent metal alkylphosphonate containing more than six carbon atoms.

Organic Films formed Using Self-Assembly Techniques

The formation of monolayer and multilayer films using the self-assembly method relies on the affinity of molecules for each other and the affinity of the molecules for surfaces. The spontaneous chemisorption of thiols on gold, organosilicon molecules on hydroxylated surfaces, and carboxylic acids on silver are all examples of self-assembly reactions. From an energetics standpoint, the self-assembling molecule can be divided into three parts - the headgroup, which forms a bond with the substrate; the alkyl chain, which provides van der Waals interactions between molecules and affects the order of the film; and the terminal group which are normally disordered at room temperatures.[33] Clearly the attraction of the molecular headgroup for the surface is the driving force behind molecular self-assembly. The disadvantage of applying self-assembled films to the investigation of two-dimensional properties results from the strong interactions that exist between the monolayer and the surface. Generally, these interactions are so strong that the properties of the self-assembled monolayer become coupled to the substrate and the monolayer becomes part of a three-dimensional structure. For example, it was demonstrated by Whitesides et al.[36] that self-assembled monolayers of docosanethiol on various gold surfaces form with

structures reflective of the respective surface to which they adhere.[37] When docosanethiol is self-assembled on Au(111) surfaces, the symmetry of sulfur atoms in the monolayer is hexagonal indicating that sulfur binds at certain hollow sites on the Au(111) surface.[37] However, when docosanethiol is self-assembled on Au(100) surfaces, the symmetry of the alkanethiol assembly is base-centered square. Whitesides determined that on the Au(100) surfaces, sulfur binds chemisorbs on both on-top and threefold hollow sites in an alternating fashion.[37] It was found that the resulting monolayers of the docosanethiols on the two different surfaces also have differences in the tilt angle of the alkyl chains.[37] This clearly indicates that the structure and properties of self-assembled monolayers are contingent upon the structure of the substrate to which they chemisorb.

As in the case of the assembly of thiols on gold, numerous investigations involving the structure of self-assembled monolayers and multilayer of organosilanes on silicon or glass have been reported.[33,38-40] The self-assembly reaction of octadecyltrichlorosilane on a hydroxylated surface is dipicted schematically in Figure 1-6. In this reaction, octadecyltrichlorosilane is dissolved in an organic solvent containing a substrate such as glass or silicon. Si-Cl bonds react with the OH groups present on the surface of the substrate and with neighboring Si-O groups to form a network of Si-O-Si Bonds.[33] van der Waals interactions between the long chain alkyl groups also occur and increase the order of the monolayer. As a result of the covalent bonds between the head group and substrate in addition to the interactions between molecules, self-assembled monolayers of alkylsilanes on glass or silicon form close-packed, ordered films on the surface of the substrate. The monolayers terminate with methyl groups which chemically modify wetting properties of the substrate.[33] The research presented in this dissertation makes use of this self-assembly reaction to obtain close-packed, highly ordered hydrophobic substrates onto which monolayers are then deposited. When monolayers of different amphiphilic molcules are deposited, via the Langmuir-Blodgett technique, onto these surface modified substrates interactions between the amphiphilic molecules and the surface are eliminated.

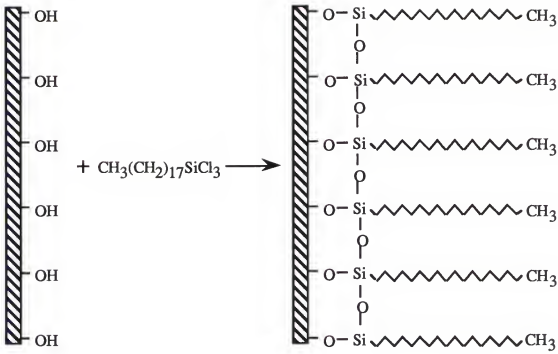

Figure 1-6. Self-Assembly of octadecyltrichlorosilane on a hydroxylated surface.

The Langmuir-Blodgett Method

Amphiphilic molecules may be organized at an air-water interface using a Langmuir-Blodgett trough. The formation of a Langmuir monolayer, developed by Irving Langmuir[41], is depicted in Figure 1-7. The procedure consists of dropping a volatile solution of an amphiphilic molecule onto a water surface contained inside a teflon 'trough' having movable teflon barriers. The solvent evaporates and the polar end of the amphiphile wants to dissolve into the water subphase; the hydrophobic end is directed away from the aqueous surface. At this stage, the molecules are separated from each other by large distances and are labeled as a two-dimensional "gas" as shown in part A of Figure 1-7.[33] The organization of the molecules on the surface of the subphase is monitored by the change in surface tension of pure water and the surface tension of water covered with a monolayer. This difference in surface tension is equivalent to the surface pressure and is

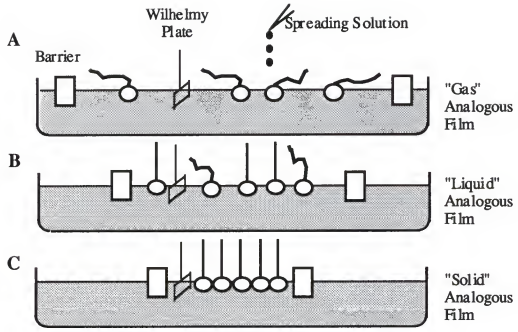

Figure 1-7. Formation of a Langmuir Monolayer at the air/water interface. A-C depict the three stages in the organization of the monolayer as monitored by the measurement of the surface pressure of the aqueous subphase.

measured using a platinum plate, more commonly known as a Wilhelmy plate, suspended from a microbalance.[42] At this stage, the barriers move and compress the molecules at the air/water interface. The molecules become closer together and undergo a phase transition from a "liquid" state, Figure 1-7B, to eventually a "solid" state where the molecules make up a closely packed and uniformly oriented monolayer[42] as illustrated in Figure 1-7C. During the formation of the Langmuir monolayer, the surface pressure is recorded as a function of the area per molecule since the total number of molecules and the area that the monolayer occupies is known. A typical plot of a pressure-area isotherm is shown in Figure 1-8. In the gas region of the pressure-area isotherm, interactions between molecules are negligible and surface pressure is low. As the molecules are compressed, interactions between molecules increase and surface pressure slowly rises. As the molecules are compressed further, surface pressure increases rapidly as the head groups and hydrophobic

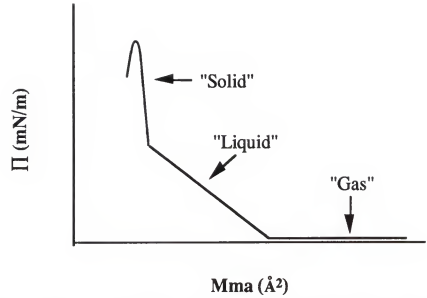

Figure 1-8. A Pressure-Area Isotherm. Typically three distinct regions are observed in the formation of a Langmuir Monolayer signified by changes in slope of the line.

portions of the molecules form a close-packed, organized monolayer.

The next stage in the Langmuir-Blodgett experiment involves the transfer of the Langmuir monolayer onto the surface of a solid support. The vertical deposition method, illustrated in Figure 1-9, is the most conventional method of transferring monolayers onto solid supports and was developed by Blodgett and Langmuir in 1937.[43] The procedure involves moving a substrate through a Langmuir monolayer which is held at a surface pressure chosen in such a manner that the monolayer will maintain its close-packed, uniformly organized structure. When the substrate is hydrophobic, as shown in Figure 1-9, the monolayer will be transferred on the down-stroke with the hydrophobic alkyl chains of the monolayer interacting with the surface. Upon withdrawal of the substrate from the subphase, hydrophilic interactions of the head-groups will occur and result in the deposition of a second monolayer onto the substrate. It is common to call the transfer of two complete monolayers onto a substrate, deposition of a Langmuir-Blodgett bilayer. Therefore, in this dissertation, a bilayer is defined as consisting of two organic portions and one inorganic portion as shown in Figure 1-10.

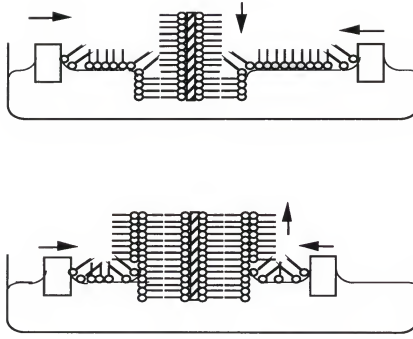

Figure 1-9. Deposition of a Langmuir Monolayer onto a Hydrophobic Substrate. Transfer of a monolayer results from the hydrophobic interactions between the substrate and the hydrophobic part of the monolyaer as the substrate is lowered through the monolayer. When the substrate is withdrawn through the air/water interface, interactions between the polar portions of the monolayer result in the transfer of a complete bilayer of a LB film.

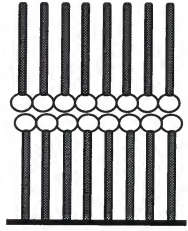

Figure 1-10. A Langmuir-Blodgett Bilayer. The sticks represent the hydrophobic alkyl groups in the bilayer and the balls represent the hydrophilic portion of the bilayer.

Saturated fatty acid molecules were the pioneer molecules used by Langmuir and Blodgett over 60 years ago[44] and have continued to maintain their popularity in this field. The literature is flooded with studies of long chain carboxylic acids and their relation to Langmuir monolayers and LB films. One of the most challenging aspects of ultrathin film research lies in the structural characterization of such minute amounts of materials. A great advancement in the area of Langmuir-Blodgett films came from the modification of surface sensitive anayltical techniques to probe the molecular structure of ultrathin films. Zasadzinski, Dutta, and Blasie were just a few of the many researchers to make significant contributions to this advancement by providing insight to the in-plane structure and morphology of LB films of fatty acid salts using high-resolution X-ray diffraction methods and scanning probe microscopy.[32,45-49] From their structural reports on Langmuir monolayers and Langmuir-Blodgett films, one may better understand how to modify variables in the LB experiment to fabricate thin films with significant control at a molecular level.

The in-plane structure of LB films of barium and lead stearate was determined using X-ray diffraction methods.[48,49] By comparison of the diffraction patterns obtained from multilayers of the films with the diffraction patterns obtained from powdered samples of lead stearate, assignment of a unit cell for the films was possible.[48] In another more direct series of investigations, Zasadzinski also assigned unit cells for LB films of many fatty acid salts using AFM. Zasadzinski's discoveries revealed that the structure of transferred LB films of fatty acid salts did not always maintain the same structure as the corresponding floating Langmuir monolayer. A number of factors can influence the structure of the transferred film. AFM studies on arachidate monolayers and Langmuir-Blodgett monolayer and multilayer films with and without divalent metal ions, exhibit disordered arrangements of the alkyl groups for those films lacking the metal ions, to organized crystalline arrangements of the alkyl groups in those films containing divalent metal ions.[45] It was also realized that the interaction of the metal ions with the carboxylate headgroups

attributed mechanically stable films regardless of substrate, deposition conditions, number of layers, and AFM imaging conditions. It was postulated that the strong interactions between the metal ions and the oxygens of the carboxylate groups provide the energetically driving force for organization.[45] In another strikingly remarkable AFM study, experiments revealed that with the substitution of Ba^{2+} for Cd^{2+} in fatty acid LB films the structural parameters of the molecular organization changed dramatically.[50] The authors speculate that the molecular areas of the fatty acid films are dictated by the size and bonding requirements of the metal ion and the alkane packing is forced to adopt the best configuration compatible with the molecular area.[50] Further AFM studies on lead and manganese carboxylate LB films revealed different molecular areas and alkyl chain packings than those of the corresponding carboxylate films containing cadmium and barium. This difference may be attributed to the stronger intralayer interactions present in the lead films, and to a smaller extent the manganese films.[32,35] A conclusion may be drawn from these thorough results: the most durable and closely packed LB film may be constructed by maximizing intralayer interactions of the divalent metals, and the alkyl chains will tilt to maximize the van der Waals interactions between them.

Theory of Low-Dimensional Magnetism

Understanding magnetic phenomena in two-dimensions continues to be a goal of materials research. The transition from magnetic exchange between two paramagnetic ions to spontaneous magnetization at some finite temperature depends on two factors: lattice dimensionality and spin dimensionality. Predictions of when to expect spontaneous magnetism in low-dimensional materials dates back to 1930 when Bloch concluded from his theory of spin waves with Heisenberg exchange, that ferromagnetism was impossible in two-dimensional systems.[51] This theory initiated much research into the magnetic behavior of systems with low lattice dimensionality. Onsager provided a proof that if magnetic exchange was anisotropic, or Ising type, spontaneous magnetization could occur

at finite temperatures in two-dimensions.[52] This was further validated by Mermin and Wagner who published a proof that ferromagnetism and antiferromagnetism cannot exist at finite temperatures for Heisenberg and XY spin interactions, but no conclusive argument could be made for Ising type exchange.[53] The theoretical predictions of when to expect a transition from short-range magnetic exchange to spontaneous long range order as a function of spin and space dimensionality are summarized in Figure 1-11.

The physical predictions were tested by many scientists investigating the magnetic behavior of many quasi two-dimensional materials. Numerous magnetic investigations have involved materials crystallizing with the K_2NiF_4 structure. For example, temperature dependent magnetic studies display two-dimensional antiferromagnetic exchange at high temperatures in K_2MnF_4, La_2CuO_4, and K_2NiF_4.[11,54-56] In each complex, a transition from short range order to long range order occurs. Although the observation of an ordered state in these quasi two-dimensional compounds seemed to oppose theoretical predictions, the transition was justified by a crossover in lattice dimensionality or spin dimensionality. This crossover property in two-dimensional layered materials is dependent upon the distance between magnetic layers and the magnetic correlation length within a single magnetic layer. A lattice dimensionality crossover will occur when the interactions between magnetic layers is larger than the correlation length within a layer. A dimensionality crossover from 2d Heisenberg to 3d Heisenberg is the driving force for an ordered state in complexes of La_2CuO_4.[55] On the other hand, when the correlation length or the size of the magnetically correlated spins is larger than the magnetic coupling between layers, a crossover in spin dimensionality is sited as the explanation for an observed transition to long range order. This is the case in K_2MnF_4 and K_2NiF_4. As the temperature is decreased, the correlation lengths increase and a transition from 2d Heisenberg to 2d Ising is predominant.[11,54,56]

The layered perovskites were also a popular choice for magnetization experiments on two-dimensional systems. Many alkylammonium metal tetrahalides were synthesized

Figure 1-11. Effects of Space Dimension and Magnetic Spin Interaction on Magnetic Transitions. Theory predicts a transition to long range magetic order at finite temperatures for only specific combinations of space and spin dimensions.

Lattice Dimensionality

Exchange Anisotropy	1D	2D	3D
Ising Jxy = 0	No Transition at T > 0 K	**Long Range** **Order at T > 0 K**	**Long Range** **Order at T > 0 K**
XY or Planar Jz = 0	No Transition at T > 0 K	No Transition at T > 0 K	**Long Range** **Order at T > 0 K**
Heisenberg Jxy = Jz	No Transition at T > 0 K	No Transition at T > 0 K	**Long Range** **Order at T > 0 K**

$$H = -2\Sigma\{J_{xy}(S_{ix}S_{jx} + S_{iy}S_{jy}) + J_zS_{iz}S_{jz}\}$$

and variations with respect to the length of the alkyl group and metal were made. Although these compounds are anisotropic, they remain part of a three-dimensional network and at low temperatures spontaneous magnetization occurs. The explanation for the observation of the transition in most cases, is attributed to the dimensionality crossover from two to three-dimensions and no theories have been disproven.

The magnetization measurements of a series of manganese alkylphosphophosphonates were performed by Day et al.[57] Static susceptibility measurements on manganese methyl, ethyl, propyl, and butylphosphonate exhibit a transition to long range order at about 15K. Manganese is a Heisenberg nucleus with S = 5/2, and the observation of spontaneous magnetization is attributed to a dimensionality crossover from two-dimensions to three-dimensions.[58] Since these solids are part of a three-dimensional crystal, a better two-dimensional system is a true monolayer where the magnetic coupling is restricted to two-dimensions.

In 1975, Pomerantz began a study of Langmuir-Blodgett films of manganese alkylcarboxylates in order to investigate magnetism in two dimensions.[59] He constructed Langmuir-Blodgett films containing spin 5/2 manganese ions which are Heisenberg in nature. The magnetic behavior of the two-dimensional film was probed with EPR spectroscopy. For the EPR experiments, sample preparation involved transferring monolayers of manganese stearate onto several quartz plates and stacking together as many plates as possible using bits of mylar as spacers between the plates.[60] Extensive electron paramagnetic resonance experiments were performed on the films and observation of antiferromagnetic exchange was reported. Evidence of a transition from short range order to long range order was cited, but no direct observation of an ordered state was achieved.[60]

Scope of Dissertation

There is currently high interest in engineering mixed organic/inorganic materials where features of the organic and inorganic components complement each other leading to

new solid-state structures and materials with composite or even new properties. Some examples of recent interest are layered inorganic solids with organic intercalates,[61,62] organic/inorganic low-dimensional solids,[9,21,63,64] zeolites and other open framework host materials with organic guests,[65,66] metal oxide mesostructures formed with the aid of organic surfactants,[67-69] and thin film heterostructures built-up from alternating layers of organic polyelectrolytes and colloidal inorganic polyions.[70,71] In some cases, a stable inorganic lattice facilitates spatial and orientational control of organic molecules. On the other hand, new inorganic lattice structures are sometimes formed resulting from cooperative interactions between the organic and inorganic components. In all cases, there is the promise of developing new materials with properties not seen in purely organic or purely inorganic solids.

The Langmuir-Blodgett technique allows for the organization of molecular assemblies at air/water interfaces. The assemblies may be transferred onto solid substrates and in favorable cases, well ordered ultrathin films are formed. Langmuir monolayers are constructed from amphiphilic molecules containing long organic groups and polar headgroups, with long chain carboxylic acids historically being the most popular choice of amphiphile. It is long been realized that metal ions added to the subphase under monolayer films of fatty acids can be incorporated into Langmuir-Blodgett monolayer and multilayer films.[44] Divalent metal ions crosslink the carboxylate groups forming a two-dimensional inorganic lattice and enhance the stability of the transferred films.[33,42,72] The addition of an inorganic extended lattice into LB films opens the possibility of introducing physical properties that are typical of the inorganic solid-state. Through recent structural studies on LB films of fatty acid salts,[32,46,73-75] it also became clear that the ionic interactions between the polar carboxylate headgroup and the metal ion often determine the destiny of the transferred film. Historically however little attention has been placed on using these favorable interactions to gain more control over the deposited film. It seems evident to utilize these favorable polar headgroup interactions found in carboxylic acid films of

amphiphilic molecules with metal ions to purposefully control and dictate the structures of LB films consisting of different amphiphilic molecules. Once it is demonstrated that crystalline inorganic extended-lattice structures may be incorporated into ultrathin films and the inorganic lattice retains its anticipated behavior, the nature of the organic portion of the films may be given functionality and the possibility exists to fabricate LB films with hybrid organic/inorganic properties.

To begin these investigations, hybrid organic/inorganic LB films in which the organic portions bear no other purpose than to isolate the inorganic layers were fabricated to determine if inorganic extended-lattice structures could be incorporated into organic films. Chapter two presents a thorough structural study of LB films of a series of divalent metal octadecylphosphonates. The Langmuir-Blodgett technique is used in conjunction with the favorable lattice energy found to be present in solid-state metal phosphonate compounds to purposefully control molecular structure and properties to form high quality, durable ultrathin organic films. It will be demonstrated that extended-lattice monolayers and multilayers of some of the metal phosphonates can be prepared using the Langmuir-Blodgett (LB) method.[76,77] The lattice energy between the metal ions and the oxygens of the phosphonate head groups, determines the structure of transferred LB films of divalent metal alkylphosphonates. The alkyl chains vary their packing, tilt angle, and tilt direction to achieve close-packing in the organic/inorganic thin films. Single layer and multilayer LB films of manganese, cadmium, cobalt, magnesium, and calcium octadecylphosphonate were prepared and the structures of the films are compared to the structures of the solid-state structures to verify that the films are isostructural with the solid-state metal organophosphonates. It will be demonstrated using the especially compelling example of the calcium octadecylphosphonate LB film that the structure of each octadecylphosphonate LB film depends on the identity of the metal ion. The strong metal/phosphonate binding interaction determines the structure of the LB films just as in the solid-state phosphonates.

To provide further evidence that organized inorganic extended-lattice structures may be incorporated into LB films, a detailed electron paramagnetic resonance (EPR) investigation was performed on LB films of manganese octadecylphosphonate and presented in chapter three. The magnetic properties of the manganese LB film are compared to the structurally analogous manganese alkylphosphonate powdered samples.

The magnetic interactions between the paramagnetic manganese ions in powered samples of a series of manganese alkylphosphonates with varying alkyl chain lengths were probed using static magnetic susceptibility measurements.[57,58] It was found that the manganese ions undergo two-dimensional Heisenberg antiferromagnetic exchange at high temperatures. At approximately 15 K a transition from short range antiferromagnetic order to one of long range order occurs and a weak ferromagnetic moment is observed.[57,58] The exhibited magnetic properties of these solids require that the inorganic layer be organized and crystalline.

Chapter three summarizes the results of an investigation using variable temperature EPR spectroscopy on a 50 bilayer LB film of manganese octadecylphosphonate. As it will be pointed out, the magnetic exchange in the manganese LB film is similar to the magnetic exchange observed in the powered manganese alkylphosphonates. From the EPR studies, the manganese LB film can best be described as a two-dimensional Heisenberg antiferromagnet. The g values of the LB film are characteristic of Mn^{2+} in a nearly cubic field and are essentially isotropic. The dependence of the EPR linewidth on sample orientation in the magnetic field is consistent with the behavior predicted for a two-dimensional lattice with antiferromagnetic Heisenberg exchange. The temperature dependence of the integrated area of the EPR signal, which is proportional to spin susceptibility is presented. A value for the antiferromagnetic exchange constant was extrapolated from the results and the value agrees closely with the exchange constants of the analogous solid-state manganese phosphonates. EPR linewidths of the manganese octadecylphosphonate LB film increase rapidly as the temperature is lowered below 30 K.

This is characteristic of a system approaching a magnetic ordering transition . Using EPR spectroscopy, an ordering transition cannot be observed since the linewidth becomes too broad and the signal is too weak to measure below 17 K.

With evidence from the EPR study of the manganese octadecylphosphonate LB film pointing to the likely occurance of a transition from short range two-dimensional Heisenberg antiferromagnetic exchange to long range order, there was desire to probe the magnetic behavior of the LB film at lower temperatures. In chapter four, static magnetic susceptibility experiments were performed on multilayer samples of manganese octadecylphosphonate LB films. In agreement with the magnetization studies of the powered manganese alkylphosphonate samples, the LB film also undergoes a transition to long range order at 13.5 K. Below the ordering temperature the manganese LB film exhibits a weak ferromagnetic moment. The weak moment in the ordered state is due to antiferromagnetic ordering where coupled nearest neighbor moments do not exactly cancel due to spin canting. These results are the first demonstration of cooperative ordering in an LB film. The LB film also displays magnetic memory below the ordering temperature. The effect is small but nevertheless this is the first observation of a magnetic LB film. The magnetic exchange is due to superexchange via the phosphonate ligand and the extended-lattice structure of the film provides sufficient structural order for magnetic ordering to take place. As a result of these magnetic investigations, it is established conclusively that extended-lattice layered structures can be incorporated into LB films and properties normally associated with solid-state inorganic structures can be incorporated into ultrathin organic films.

It is well established[1] that any magnetic interlayer interactions that occur in quasi two-dimensional solids act to increase the ordering temperature and any nonmagnetic impurities cause a suppression in the ordering temperature.[55] In chapter five the manganese octadecylphosphonate LB films are manipulated in such a way as to investigate the importance of the interlayer magnetic exchange. In the pure manganese LB films,

where ordering occurs at 13.5 K, the separation between successive manganese layers is about 50Å and it is predicted that any exchange that occurs between layers is minimal. In order to accurately asses this prediction, LB films of alternating layers of manganese and cadmium octadecylphosphonate were prepared.

Since cadmium is diamagnetic, the layers of cadmium octadecylphosphonate act as nonfunctional spacers in these new expanded manganese films. The separation between adjacent manganese layers is now increased from 50Å to 100Å. Magnetic susceptibility measurements performed on the expanded films resulted in an ordering temperature of 10.5 K, about 3 K lower than the ordering temperature of the pure manganese LB films.

In addition, Langmuir-Blodgett films of manganese octadecylphosphonate with manganese layers separated by two layers of cadmium octadecylphosphonate were also prepared. In these films, the distance between manganese layers is now tripled relative to the pure manganese LB film. Again, magnetic measurements illustrate an ordering temperature at 10.5 K. It seems unlikely that the suppression in the transition temperature in the two expanded manganese LB films relative to the pure manganese LB film is due to interlayer coupling since the interlayer distance in the pure manganese film is so large. Instead a more likely explanation of the temperature suppresion is due to small nonmagnetic impurities in the manganese layers of the alternating manganese/cadmium films. These impurities due to cadmium ions in the manganese layers, act to break up the domains of manganese spins. With the decrease in the correlation length of the manganese spins, a reduction in the ordering temperature is expected. To provide further evidence of this explanation magnetic measurements were performed on two additional LB samples. The first sample contained 13% Cd mixed into the manganese layers. With the large amount of nonmagnetic impurities, the correlation lengths of the manganese spins was so small no transition to long range order occured. Instead, the manganese spins acted independently and the results were comparable to a normal paramagnet. In a second sample, 5% Cd was mixed into the manganese layers. Magnetization measurements revealed a supression of

the ordering temperature. The results of chapter five illustrate that the magnetic behavior of the LB films obeys the predictions set by basic theories of magnetism, but most importantly it demonstrates that inorganic properties observed in solid-state materials may be incorporated into Langmuir-Blodgett films.

CHAPTER 2
LANGMUIR-BLODGETT FILMS OF KNOWN LAYERED SOLIDS: PREPARATION AND STRUCTURAL PROPERTIES OF OCTADECYLPHOSPHONATE BILAYERS WITH DIVALENT METALS

Introduction

The Langmuir-Blodgett technique[33,42,43,72,78] is one of the oldest and most elegant approaches known that allows researchers to purposefully arrange molecules into organized assemblies. Molecules, usually amphiphiles, are first compressed to a close-packed monolayer at a water surface followed by transfer of the assembly as a monolayer to a solid support. Multilayer films are formed through repeated deposition cycles. While the LB method is normally considered a technique for organizing organic molecules, inorganic ions are often incorporated into transferred films.[33,43,72] The metal ions crosslink charged molecules and enhance the films' stability and processibility, but they are generally thought of as passive elements in the otherwise organic assemblies. While there are recent studies that show how the identity of the inorganic ions can influence the LB film structure,[32] there has been relatively little effort by researchers to control the structure and function of the inorganic component of LB films.[33,72] If the inorganic network can be purposefully developed, then the alternating hydrophobic and hydrophilic layered structure of LB films, coupled with the ability to control layer-by-layer deposition, should provide a unique opportunity to explore the fabrication of mixed organic/inorganic layered solids and thin films.

The approach that is used to investigate control of the inorganic component of LB films is to base the films on known inorganic layered structures and incorporate inorganic extended lattice structures into the hydrophilic portion of the LB assemblies.[76,77,79] There are numerous examples of inorganic and mixed organic/inorganic layered solids,[9,80] and

the objective is to use LB methods to prepare examples of these extended lattice inorganic layers. If the inorganic lattice favors a layered structure it might complement the layered nature of organic LB film assemblies. These concepts were previously demonstrated[76,77,79] in the characterization of LB films of zirconium octadecylphosphonate and manganese octadecylphosphonate which are each analogs of known metal phosphonate layered solids.[15,17,21,81] Although the tetravalent and divalent metal phosphonate solid-state structures are slightly different,[15,17,21,81] these solids are all characterized by sheets of metal ions that are bonded above and below the metal ion plane by layers of the organophosphonates as illustrated by the cartoon shown in Figure 2-1. The phosphonate ligands bridge metal ions forming the extended lattice layers, and adjacent layers are separated by van der Waals interactions between the organic groups. The zirconium phosphonate and manganese phosphonate LB films have been shown to have the same inorganic lattice structure as the analogous solids.[76,77,79]

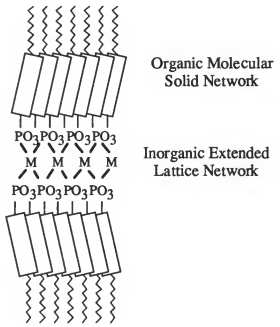

Figure 2-1. Illustration of a Metal Organophosphonate Compound. In the solid-state, these materials consist of two dimensional arrays of organic molecular networks separated by inorganic extended lattice networks.

This chapter describes LB films modeled after divalent metal organophosphonates. Thorough structural studies by Mallouk and co-workers[13-15,21,22] and Cao and coworkers[16] have identified two series of solid-state divalent metal organophosphonates, $M(O_3PR)\cdot H_2O$ (M = Mg, Mn, Zn, Ca, Co, Cd; R=n-alkyl, aryl group) and $M(HO_3PR)_2$ (M = Ca). Each forms a layered structure and interlayer distances vary to accommodate the different R groups. For M=Mg, Mn, Co, and Zn in the first series, the layered phosphonates are isostructural, crystallizing in an orthorhombic space group.[14,15] Each phosphonate group bridges four metal ions and the metal ions are coordinated by five oxygens from four different phosphonate groups. The distorted octahedral coordination of the metal ion is completed by a water of hydration as seen in Figure 2-2 for the crystal structure of cadmium methylphosphonate.[16] For M=Ca or Cd in the same series, a structure of slightly lower symmetry is adopted.[13,14,16] In the second series, calcium forms 1:2 salts with alkylphosphonates having alkyl groups containing five carbon atoms or greater as illustrated in Figure 2-3.[13,14]

This chapter will illustrate how the LB approach for depositing metal phosphonate films is quite general and offers a compelling example of how the choice of metal ion can be used to control the structure of the deposited LB films. The detailed description of the preparation and characterization of octadecylphosphonate LB films with a series of divalent metals including Mn^{2+}, Mg^{2+}, Cd^{2+}, Co^{2+} and Ca^{2+} will be presented. While different structures are observed, each LB film will be shown to adopt the same metal-phosphonate binding as the known solid-state analogs. The Mn^{2+}, Cd^{2+}, Co^{2+} and Mg^{2+} octadecylphosphonate LB films form $M(O_3PR)\cdot H_2O$ structures, and the calcium octadecylphosphonate LB film forms with a 1:2 metal to phosphonate stoichiometry and formula $Ca(HO_3PR)_2$. The different structures demonstrate the important role that the inorganic extended lattice plays in organizing the LB films and that the metal phosphonate LB film structure can be controlled by choice of metal ion.

Figure 2-2. X-ray crystal structure of cadmium methylphosphonate, $Cd(O_3PCH_3)\cdot H_2O$. (A) Packing diagram, and (B) Cadmium coordination. Structural coordinates taken from reference 16.

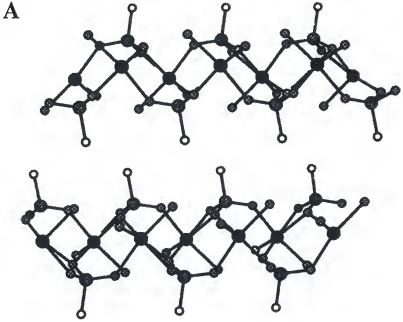
A
B
O
Cd
P

Figure 2-3. X-ray crystal structure of calcium hexylphosphonate, $Ca(HO_3PC_6H_{13})_2$. (A) Packing diagram, and (B) calcium coordination. Structural coordinates taken from reference 13.

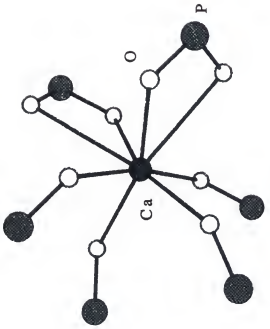

B

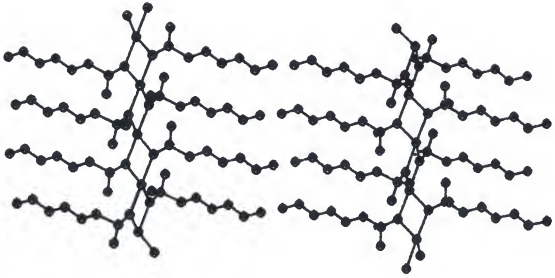

A

Experimental Section

Materials

All chemicals were purchased and used without further purification. Octadecylphosphonic Acid, $CH_3(CH_2)_{17}P(O)(OH)_2$, 98% was purchased from Alfa Aesar (Ward Hill, MA). $MnCl_2{\cdot}4H_2O$ (99.6%), $CoCl_2{\cdot}6H_2O$ (99%), and $CaCl_2$ (97.8%) were purchased from Fisher Scientific (Fair Lawn, NJ). $CdCl_2{\cdot}2.5H_2O$ was obtained from Aldrich (Milwaukee, Wisconsin). $Mg(NO_3)_2{\cdot}6H_2O$ was obtained from Mallinckrodt, Inc. (Paris, Kentucky). Octadecyltrichlorosilane (OTS, $C_{18}H_{37}SiCl_3$, 95%) was purchased from Aldrich and stored under N_2. A Barnstead Nanopure (Boston, MA) purification system produced water with an average resistivity of 18 MΩ-cm for all experiments.

Substrate Preparation and Deposition Procedure

Single crystal (100) silicon wafers, purchased from Semiconductor Processing Company (Boston, MA), were used as deposition substrates for XPS and ellipsometry measurements. Glass slides, (Buehler; Lake Bluff, IL) were the substrates in the XRD experiments. The silicon and glass substrates were cleaned using the RCA cleaning procedure[82] then dried under N_2. Germanium attenuated-total-reflectance (ATR) crystals, (45° 50mm x 10mm x 3mm) purchased from Wilmad Glass (Buena, NJ), were used as substrates for the infrared experiments. Octadecyltrichlorosilane (OTS) was self-assembled[39,83] onto the substrates to make them hydrophobic. The clean substrates were placed in a 2% solution of OTS in hexadecane for 30 minutes, rinsed with chloroform to remove any excess hexadecane, and dried under a stream of nitrogen.

Divalent metal octadecylphosphonate Langmuir-Blodgett films were prepared by spreading octadecylphosphonic acid onto an aqueous subphase containing a salt of the

appropriate metal at a concentration of 5 x 10^{-4} M. The pH of the subphase was adjusted appropriately using HCl or KOH. Target pressures, barrier speeds, and subphase pH varied depending on the metal used as recorded in Table 2-1.

Table 2-1. Deposition conditions for the preparation of metal octadecylphosphonate LB films.

LB Film[a]	Subphase pH	Target Pressure (mN/m)
$Mn(O_3PC_{18}H_{37})\cdot H_2O$	5.2 - 5.6	20
$Cd(O_3PC_{18}H_{37})\cdot H_2O$	4.2 - 5.0	17
$Mg(O_3PC_{18}H_{37})\cdot H_2O$	7.4 - 7.6	17
$Ca(HO_3PC_{18}H_{37})_2$	7.0 - 8.10	17
$Co(HO_3PC_{18}H_{37})$	5.5-5.8	17

a) Barrier speeds = 5mm/min on the upstroke; 8mm/min on the downstroke.

Instrumentation

The LB films were prepared using a KSV (Stratford, CT) 3000 trough modified to operate with double barriers. The surface pressure was measured with a platinum Wilhelmy plate suspended from a KSV microbalance.

Infrared spectra were recorded with a Mattson Instruments (Madison, WI) Research Series-1 FTIR spectrometer using a narrow-band mercury cadmium telluride detector. LB films were deposited on OTS-covered Ge ATR crystals and a Harrick (Ossining, NY) TMP stage was used for the ATR experiments. Polarized FTIR-ATR spectra were taken with s- and p- polarized light. All ATR spectra consisted of 1000 scans at 2.0 cm^{-1} resolution and were referenced to the OTS-covered Ge ATR crystal or the appropriate s- or p- polarized background.

X-ray photoelectron spectra were obtained using a Perkin-Elmer (Eden Prairie, MN) PHI 5000 Series spectrometer. All spectra were taken using the Mg K_α line source at 1253.6 eV. The spectrometer has a typical resolution of 2.0 eV, with anode voltage and

power settings of 15 kV and 300 W, respectively. Typical operating pressure was 5×10^{-9} atm. Survey scans were performed at a 45° take-off angle with a pass energy of 89.45 eV. Multiplex scans, 140 scans over each peak, were run over a 20-30 eV range with a pass energy of 35.75 eV. The observed relative intensities were determined from experimental peak areas normalized with atomic and instrument sensitivity factors.[84,85]

X-ray diffraction was performed with a Philips APD 3720 X-Ray Powder Diffractometer using the Cu K_α line, $\lambda = 1.54$ Å, as the X-ray source.

Ellipsometry measurements were performed on a Rudolph Instruments (Fairfield, NJ) Series 431A Universal Ellipsometer using a 70° angle of incidence with a helium-neon laser, $\lambda = 632.8$ nm, as the source.

Results and Discussion

Film Deposition

The divalent metal octadecylphosphonate LB films are transferred onto solid surfaces by compressing the monolayer to an optimum pressure, Table 2-1, then lowering a hydrophobic substrate through the film at 8mm/min, transferring the film in a tail-to-tail fashion on the down-stroke. The substrate is then raised from the subphase through the monolayer at a speed of 5mm/min, forming a head-to-head bilayer as demonstrated in Figure 2-4. All of the films discussed in this paper have been transferred onto solid supports made hydrophobic with a self-assembled monolayer of OTS. Slow deposition speeds for the up-stroke allow draining of the water from the film and aid in the crystallization of the inorganic lattice. To prepare crystalline LB films of the phosphonates on solid surfaces, the optimum pH of the subphase depends on the identity of the metal ion; Table 2-1. The metal phosphonates are soluble in acid solutions so if the subphase pH is too low, metal ions are not incorporated into the Langmuir monolayer, but if the subphase pH is too high phosphonate groups cross-link the M^{+2} ions at the air/water interface

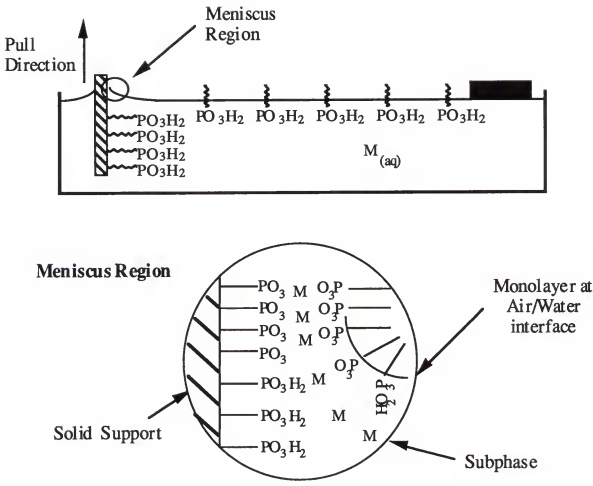

Figure 2-4. Deposition of a divalent metal alkylphosphonate Langmuir-Blodgett film. Interactions between the hydrophobic substrate and the hydrophobic part of the Langmuir monolayer result in the transfer of one layer of the phosphonic acid. Bonding of the metal ions in the subphase to the oxygens of the phosphonate groups results in the incorporation of metal ions in the LB film and upon withdrawal of the substrate from the subphase, a second layer of alkylphosphonate is deposited onto the substrate.

making the Langmuir monolayer too rigid to transfer. Therefore, the optimum subphase pH is the highest possible pH at which the monolayer is not too rigid to transfer. Multilayers of the metal phosphonate films are not formed by continuous deposition of the films because the Langmuir monolayer becomes too rigid with time. Instead, one bilayer is transferred to a substrate, then the monolayer is removed from the water surface and a new octadecylphosphonic acid monolayer is formed. For each of the metal phosphonate systems studied, this deposition technique produces mulitlayer films with each successive transfer having a transfer ratio of 1.0±0.1.

X-ray photoelectron Spectroscopy

In the XPS experiment, photons of sufficiently high energy strike a sample and ionize atoms in the sample. The kinetic energy, KE, of the ejected electrons depends on the energy of the incoming photons, hν, and the binding energy, BE, of the atom from which the electron originated according to the Einstein photoelectric law: $KE = h\nu - BE$.[86] Since elements have characteristic binding energies, the position of the observed peaks in the XPS spectrum may be used to identify the elements in the sample. Figure 2-5 shows the XPS survey and multiplex spectra from one bilayer of a magnesium octadecylphosphonate LB film. In all LB films, elemental analyses determined by XPS, reveals that the only atoms present in each are carbon, oxygen, phosphorus, and the appropriate metal.

Obtaining quantitative information from the XPS experiment, however, is not as straightforward. Many instrumental and experiemental factors play a role in determining the intensity of each peak in the XPS spectrum.[87] As illustrated in Figure 2-6, incoming X-rays having intensity I_o enter the surface of the sample and penetrate to some depth, d_m, below the surface where there exist N_i atoms of element i. Electrons from these elements will be removed from each occupied orbital. The probability for photoejection from each orbital, the photoionization cross section, σ, is different for each orbital and different for a given orbital in different elements. Tables of cross section values have been compiled from

Figure 2-5. (A) XPS survey spectrum from one bilayer of a magnesium octadecylphosphonate LB film. (B) XPS multiplex spectrum of a single bilayer of magnesium octadecylphosphonate. The magnesium 2p and phosphorus 2p signals are shown. Integrated intensities are consistent with a 1:1 Mg to P ratio after accounting for the film geometry, photoelectron energies, and the appropriate elemental and instrumental sensitivity factors.

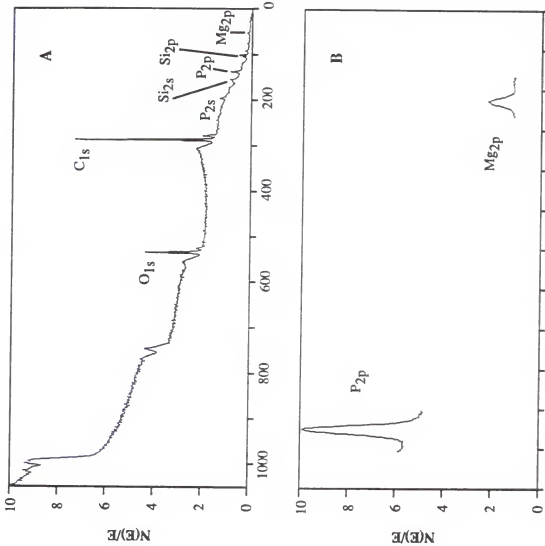
A
B
N(E)/E
Binding Energy (eV)
O1s
C1s
Si2s
Si2p
P2p
P2s
Mg2p
P2p
Mg2p

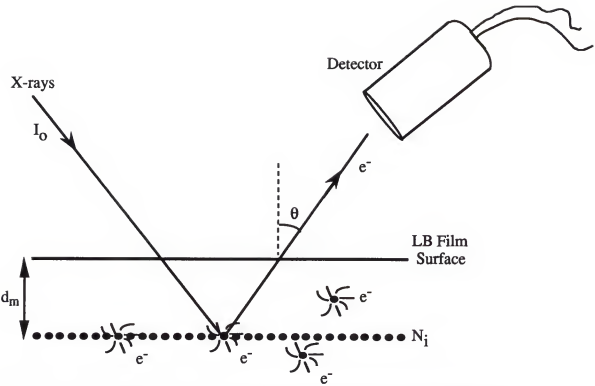

Figure 2-6. Illustration of the XPS Experiment and the Factors that Influence Quanification of the XPS Spectrum.

experimental measurements of relative peak areas on materials of known compostition.[84] Electrons from atomic energy levels will be emitted in all directions as shown in Figure 2-6, but only those aimed at the detector will be counted. The fraction aimed at the detector will be $A/4\pi^2$, where A is the area of the sample. In order to be detected, the electrons must travel through the sample and escape. The inelastic mean free path of the electrons is defined as the distance over which about 60% of the electrons can travel before losing energy in collisions with other electrons.[87] The amount of electrons reaching the detector, λ_i, depends exponentially on the inelastic mean free path of the electrons, λ_e, where $\lambda_i = e^{dm/\lambda_e \cos\theta}$. Since the detector reports only a fraction of the photoelectrons that arrive, D, the integrated area of the XPS signal also depends on this quantity. The total intensity, I, for element i, is equal to the product of all the above factors: $I_i = I_o \theta d N_i \sigma (A/4\pi^2) \lambda_i D$.[87] The factors related to instrument geometry, X-ray flux, and photoelectron production remain constant and are often incorporated into manufacturers

tables of atomic sensitivity factors. The peak areas in the octadecylphosphonate LB films have been integrated and corrected with atomic sensitivity factors[84,85] to yield the observed relative intensities for each element, as summarized in Table 2-2.

Table 2-2. Relative Intensities[a] of the Metal and Phosphorus XPS Signals for Single Bilayers of the Divalent Metal Octadecylphosphonate LB Films.

LB Film	XPS Peak	Observed Relative Intensity (±3%)	Calculated Relative Intensity[b] (%)
$Mn(O_3PC_{18}H_{37})\cdot H_2O$	Mn_{2p}	37	40
	P_{2p}	63	60
$Cd(O_3PC_{18}H_{37})\cdot H_2O$	Cd_{3d}	44	47
	P_{2p}	56	53
$Mg(O_3PC_{18}H_{37})\cdot H_2O$	Mg_{2p}	47	51
	P_{2p}	53	49
$Co(O_3PC_{18}H_{37})H_2O$	Co_{2p}	38	38
	P_{2p}	62	62
$Ca(HO_3PC_{18}H_{37})_2$	Ca_{2p}	29	32
	P_{2p}	71	68

a) Intensities are reported as the percentage of the sum of the integrated areas of the metal and phosphorus peaks after correcting for elemental sensitivity factors.
b) Assuming a layered structure, using a model described in reference.[88]

Atomic sensitivity factors, I^{∞}, will have different values for different peaks of different elements. Peaks measured for various elements having considerably different energies will have significantly different inelastic mean free paths. As a consequence, the relative intensity of the peaks will not reflect the appropriate concentrations of the elements in the sample since the sampled volume of those electrons with a larger mean free path will be larger. A model was derived to accurately predict the expected relative XPS signal intensities for the elements based on the layered film geometry.[88] Seah and Dench developed an equation to estimate the inelastic mean free path of a photoelectron in an organic film, $\lambda_e = 10[49/(KE^2) + 0.11(KE)^{0.5}]$ (Å).[89] The intensity of an element, A, is given by an attenuation equation:[87]

$$I_A = I_A^{\infty} \exp\left[\frac{-dm}{\lambda e \sin\theta}\right]$$

where is I_A^{∞} the atomic sensitivity factor and d_m is the overlayer thickness. The relative intensity for element A is given by:[87]

$$I_A = \frac{I_A^{\infty} \sum \exp\left[\frac{-dm}{\lambda e, A(\sin\theta)}\right]}{I_A^{\infty} \sum \exp\left[\frac{-dm}{\lambda e, A(\sin\theta)}\right] + I_B^{\infty} \sum \exp\left[\frac{-dm}{\lambda e, B(\sin\theta)}\right] + \ldots}$$

The overlayer thicknesses depend on the position of the atoms in the sample and may be estimated from the interatomic distances as illustrated in Figure 2-7.

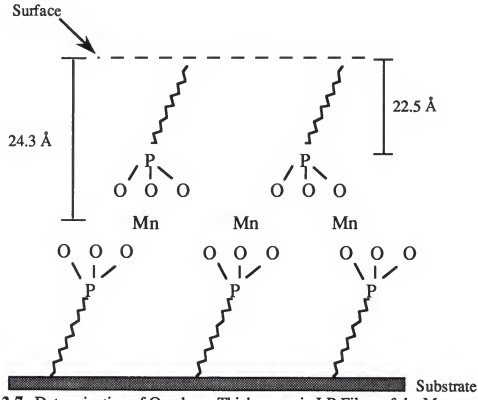

Figure 2-7. Determination of Overlayer Thicknesses in LB Films of the Manganese Octadecylphosphonates.

For the Mn^{2+}, Cd^{2+}, Co^{2+} and Mg^{2+} octadecylphosphonate LB films, the calculated ratios assume the 1:1 metal to phosphorus stoichiometry present in the $M(O_3PR)\cdot H_2O$ solid-state phases. Table 2-2 compares the calculated metal phosphorus ratios with the experimentally

observed ratios. Within experimental uncertainty (±3%), the observed ratios for the Mn^{2+}, Cd^{2+}, Co^{2+} and Mg^{2+} films are consistent with the bulk metal phosphonate stoichiometry. Elemental analysis of calcium octadecylphosphonate LB films via XPS reveals a calcium to phosphorus ratio of 1:2. In the solid-state, calcium alkylphosphonates form two layered phases with differing stoichiometries that depend on the length of the alkyl chain.[13,14] Salts with a 1:1 calcium phosphonate stoichiometry, $Ca(O_3PC_nH_{2n+1})\cdot H_2O$, form when n = 1-5; and 1:2 calcium phoshonates, $Ca(HO_3PC_nH_{2n+1})_2$, form for n > 5.[13,14] The XPS findings for the calcium phosphonate LB films are consistent with the stiochiometry observed in the solid-state calcium phosphonate compounds containing long chain hydrocarbons.

Ellipsometry and X-ray Diffraction

X-ray diffraction illustrates the layered nature of the LB films. The X-ray diffraction pattern obtained from a 15 bilayer cadmium octadecylphosphonate LB film is shown in Figure 2-8 where several orders of 00*l* reflections are observed. Interlayer spacings derived from Figure 2-8 and similar diffraction patterns for the manganese, magnesium, cobalt and calcium octadecylphosphonate LB films are summarized in Table 2-3. Interlayer thicknesses range from 46.7 - 48.5 Å which are reasonable for octadecylphosphonate bilayers.[77]

The depostition of multilayered films was followed by ellipsometry to ensure that a consistent amount of material is transferred with each bilayer. For all of the LB films, the thickness increases linearly with the number of layers, indicating that the same amount of material is being transferred to the OTS covered silicon substrate after each deposition cycle. A plot of LB film thickness as a function of the number of layers for cobalt octadecylphosphonate is shown in Figure 2-9 where the solid line is a linear fit to the data. The cobalt behavior is representative of all the films. Ellipsometry relates the thickness and refractive index of a thin homogeneous film to measurable parameters, Δ and Ψ,[33] where

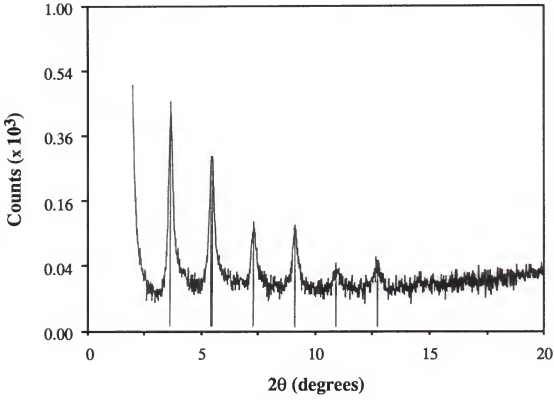

Figure 2-8. X-ray diffraction from 15 bilayers of a cadmium octadecylphosphonate LB film.

Table 2-3. Interlayer Spacings,[a] Indices of Refraction,[b] and Alkyl Chain Tilt Angles[c] for the Divalent Metal Octadecylphosphonate LB Films.

LB Film	Interlayer Spacing (Å) (±0.2Å)	Refractive Index	Tilt Angle (degrees)
$Mn(O_3PC_{18}H_{37})\cdot H_2O$	48.5	1.60	32
$Cd(O_3PC_{18}H_{37})\cdot H_2O$	48.2	1.55	36
$Mg(O_3PC_{18}H_{37})\cdot H_2O$	47.6	1.62	40
$Co(O_3PC_{18}H_{37})\cdot H_2O$	47.2	1.58	40
$Ca(HO_3PC_{18}H_{37})_2$	46.7	1.59	42

a) Determined by X-ray diffraction from films of 15 Bilayers.
b) Determined by ellipsometry.
c) Tilt angle of the alkyl chain with respect to the film normal, determined by measuring the $\nu_a(CH_2)$ band in two polarizations using ATR-FTIR.

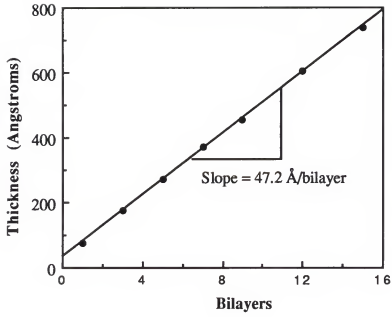

Figure 2-9. Ellipsometric data for a cobalt octadecylphosphonate LB film. The thickness of the OTS layer and oxide layer on the silicon wafer has not been accounted for,giving rise to the non-zero thickness intercept.

the angles Δ and Ψ give the change in phase and change in amplitude of plane-polarized light respectively, of light reflected off the film. Data obtained from ellipsometry were used in conjunction with data from the X-ray studies to calculate refractive indices of the organic films. Since interlayer distances obtained from X-ray diffraction are independent of optical constants, the value of the refractive index of the film was varied until the ellipsometric thicknesses agreed with interlayer thicknesses determined from X-ray diffraction. Refractive indices determined for the films range from 1.55 to 1.62, and the results are summarized in Table 2-3. Refractive indices for organic monolayers are often estimated to be 1.5,[90] based on the assumption that the monolayer is crystalline and its refractive index should be similar to polyethylene 1.49-1.55.[33] The introduction of metal ions should increase the refractive index of an organic film, thus substantiating the higher refractive indices obtained for our LB films relative to those of pure polyethylene films. The values

determined for the LB films are comparable to the refractive index of 1.54 previously measured for solid-state hafnium-1,10-decanediylbis(phosphonate).[30]

FTIR Spectroscopy

Figure 2-10 shows the FTIR spectra from 1000-4000 cm^{-1} of each of the divalent metal octadecylphosphonate films . Peaks at 2955, 2918, and 2850 cm^{-1} are assigned to the asymmetric methyl ($\nu_a(CH_3)$), asymmetric methylene ($\nu_a(CH_2)$), and symmetric methylene ($\nu_s(CH_2)$) stretches, respectively of the octadecyl chain. It has been shown that the position and shape of the $\nu_a(CH_2)$ and $\nu_s(CH_2)$ absorption bands reflect the conformational order and packing of the aliphatic chains in monolayers.[39,91,92] For long-chain hydrocarbons such as *n*-alkylthiols or polyethylene the energy of the $\nu_a(CH_2)$ band ranges from 2918-2920 cm^{-1} when the aliphatic chain is in an all-trans conformation, to 2924-2928 cm^{-1} when a "liquid-like" alkane contains a large percentage of gauche bonds.[39,91] The observed position of the $\nu_a(CH_2)$ IR band at 2918 cm^{-1} in each divalent metal octadecylphosphonate LB film implies the alkyl chains are fully extended with all-trans conformation. The $\nu_s(CH_2)$ band is also an indicator of the state of the hydrocarbon chains. This band is particularly sensitive to the average local environment of an individual chain within the monolayer indicating the density of packing of the monolayer.[91,92] The peak position of the $\nu_s(CH_2)$ band for crystalline hydrocarbons lies at 2850 cm^{-1} and shifts to higher energies, 2856 cm^{-1}, as the hydrocarbon chains become less close-packed.[91] The appearance of the $\nu_s(CH_2)$ band at 2850 cm^{-1} for each ocadecylphosphonate LB system is consistent with high density, crystalline-like phases in the monolayers. The full width at half maximum, FWHM, of the $\nu_a(CH_2)$ absorption band is another measure of the conformational order of the alkyl chains in the films,[39,91] where an organized close-packed monolayer gives a FWHM of 17 cm^{-1} and a randomly oriented film can result in a FWHM of greater than 35 cm^{-1}.[77,93] A FWHM of 17 cm^{-1} of the $\nu_a(CH_2)$ bands in each of the divalent metal phosphonate LB films is consistent with the peak-position analyses and

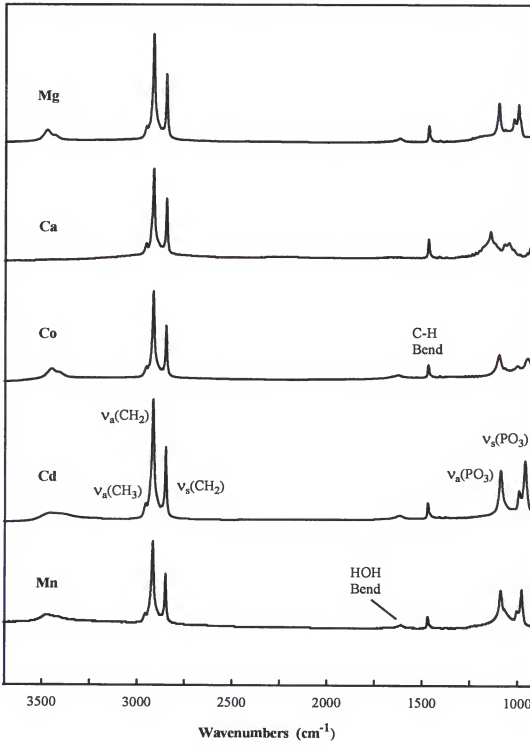

Figure 2-10. FTIR spectra from 10 bilayer LB films of magnesium, calcium, cobalt, cadmium, and manganese octadecylphosphonate.

indicates crystal-like organization of the all-trans alkyl chains. The position and shape of these hydrocarbon absorption stretching modes do not change with the deposition of additional bilayers indicating that the films maintain their structure with each succesive transfer.

The appearance of two unresolved bands at approximately 3400 cm^{-1} and a band at 1608 cm^{-1} in the IR spectra of all but the calcium octadecylphosphonate LB films indicates the presence of lattice water in the films. Lattice water absorbs at 3550-3200 cm^{-1} and at 1630-1600 cm^{-1} due to OH stretching and HOH bending modes, respectively.[94] In bulk manganese, cadmium, magnesium, and cobalt alkylphosphontes, each metal ion is bound by five oxygen atoms from the phosphonate anions and oxygen from water fills the sixth coordination site.[2,3,5] For the LB films formed with these metal ions, the intensity of the water bending mode was followed as successive bilayers were transferred to a Ge ATR crystal, Figure 2-11. A linear increase in area of the water bending mode suggests that water is stoichiometrically incorporated into the lattice and is consistent with coordination of water to the metal ions. In addition, the relative intensities of the water bending modes versus the PO_3^{2-} stretching modes in the LB films is similar to the relative intensities seen in the powdered solids. This further suggests that the coordinated water is included in the metal-phosphonate lattice of the LB film, as it is in the analogous solid-state metal phosphonates.

The absense of the water modes in the calcium film is further evidence that the calcium octadecylphosphonate LB film forms the same structure as the 1:2 calcium phosphorus solid-state phase. The main differences in the structure between solid-state calcium organophosphonates with a 1:1 calcium phosphonate stoichiometry and those with a 2:1 calcium phosphorus ratio lie in the coordination environment of the calcium ion. Calcium ions in the 1:1 salts have an approximately pentagonal-bipyramidal coordination bound by 7 oxygens, one of which is a water of hydration.[13] In the 1:2 calcium salts, calcium atoms are bound by eight oxygens from RPO_3H^- groups resulting in a distorted

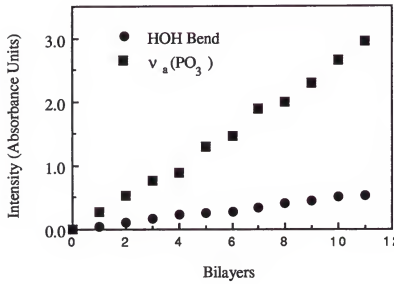

Figure 2-11. Intensity of the $\nu_a(PO_3^{2-})$ and HOH bend as a function of multilayers for the deposition of cadmium octadecylphosphonate LB film. The linear increase in the bands indicates the composition of the film is maintanined throughout the deposition process. A linear increase in the intensity of the water bending mode is evidence for the stoichiometric incorporation of water into the film.

environment. In these compounds, the hydroxyl group of RPO_3H^- is not coordinated to calcium and no water is bound to the calcium ions.[13] The absence of the ν(OH) and HOH bend absorptions in the LB film of calcium octadecylphosphonate suggests that the film structure is more like the 1:2 salt. To make additional structural comparisons, the IR spectra of the phosphonate LB films were compared to the IR spectra of solid-state metal alkylphosphonates. To illustrate, the 900-1800 cm^{-1} region of the infrared spectra for a powder sample of cadmium ethylphosphonate and cadmium octadecylphosphonate LB film are compared in Figure 2-12. Progressions of IR peaks in the 1175-1400 cm^{-1} region are assigned to CH_2 rocking and wagging modes of all-trans alkyl chains[95] for both the LB film of cadmium octadecylphosphonate and solid-state cadmium ethylphosphonate. Also common to both solid-state alkylphosphonates and the analogous LB films are small

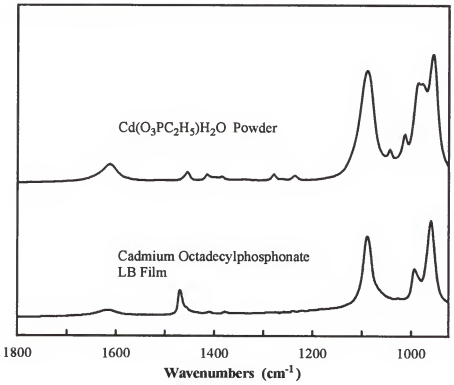

Figure 2-12. FTIR comparison of cadmium ethylphosphonate powder and cadmium octadecylphosphonate LB film. The position of the phosphonate stretching bands in the two materials is an indicator of the structural similarities.

methylene scissor deformation bands observed at 1467 and 1410 cm^{-1}. The latter band corresponds to the CH_2 group adjacent to the phosphonate group.[96,97] The absence of a strong P=O stretch[96,98] in the 1350-1250 cm^{-1} region or the 1250-1110 cm^{-1} region for free and hydrogen bonded modes, respectively, indicates that all of the phosphonate groups are ionized in the LB film as they are in the solid-state sample. On the other hand, the PO_3^{2-} stretching modes are strong and well resolved in both the LB films and powdered solids. In the IR spectrum of the LB film shown in figure 2-12, the band at 1089 cm^{-1} is assigned to the asymmetric PO_3^{2-} stretch and bands at 992 cm^{-1} and 960 cm^{-1} are the PO_3^{2-} symmetric stretches, split as a result of the lower than C_{3v} local symmetry of the phosphonate groups. The analogous bands appear at 1089 cm^{-1}, 984 cm^{-1}, and 957 cm^{-1} in the cadmium ethylphosphonate powder. The PO_3^{2-} stretching modes are very sensitive to local symmetry,[13] and the close agreement between the frequencies observed for the LB

film and those seen for the powdered solids indicates that the LB films have the same phosphorus-oxygen-metal-water extended lattice network as the solid compounds. The frequencies of the PO_3^{2-} stretching modes for each of the LB films are listed in Table 2-4 along with the frequencies observed in analogous solid-state samples. Like the cadmium case, the phosphonate binding in the manganese, cobalt, and magnesium phosphonate films is similar to the corresponding solid-state $M(O_3PR)\cdot H_2O$ phase.

Table 2-4. Comparison of the Infrared $\nu(PO_3^{2-})$ Frequencies of Powders and LB films of Divalent Metal alkylphosphonates.

Compound	$\nu_a(PO_3^{2-})$ (cm^{-1})	$\nu_s(PO_3^{2-})$ (cm^{-1})
$Mn(O_3PC_2H_5)\cdot H_2O$[a]	1087	1017, 988, 964
$Mn(O_3PC_{18}H_{37})\cdot H_2O$[b]	1087	1003, 977
$Cd(O_3PC_2H_5)\cdot H_2O$[a]	1089	984, 957
$Cd(O_3PC_{18}H_{37})\cdot H_2O$[b]	1089	992, 960
$Mg(O_3PC_{18}H_{37})\cdot H_2O$[b]	1102	1024, 999
$Ca(O_3PC_2H_5)\cdot H_2O$[a]	1093	1026, 993
$Ca(HO_3PC_{10}H_{21})_2$[a]	1146	1072, 1045
$Ca(HO_3PC_{18}H_{37})_2$[b]	1146	1072, 1045

a) Powder sample, measured as a KBr pellet.
b) LB film, measured on Ge ATR crystal.

The IR spectrum of the calcium octadecylphosphonate LB film is compared to the IR spectra of calcium decylphosphonate and calcium ethylphosphonate in Figure 2-13. There are differences in the P-O stretching region of the two solid-state calcium phosphonate compounds arising from the different structures of the two phases. The P-O stretching region of the calcium phosphonate LB film is remarkably similar to that of calcium decylphosphonate. This result, in agreement with XPS data, is conclusive evidence that the structure of the calcium octadecylphosphonate film fabricated on the LB trough is similar to the calcium alkylphosphonate solid-state compounds of molecular formula, $Ca(HO_3PC_nH_{2n+1})_2$.

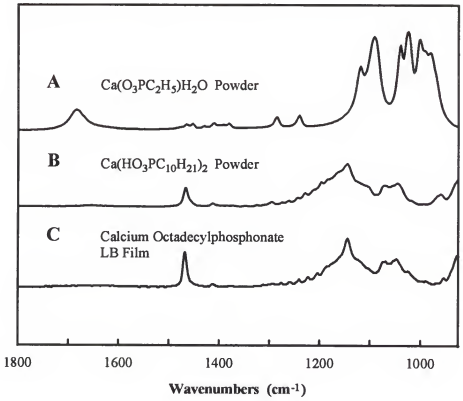

Figure 2-13. FTIR comparison of solid-state calcium ethylphosphonate, $Ca(O_3PC_2H_5)\cdot H_2O$; (B) calcium decylphosphonate $Ca(HO_3PC_{10}H_{21})_2$, powder; and (C) an LB film of calcium octadecylphosphonate. The similarity of the spectra of the solid-state calcium decylphosphonate and the calcium phosphonate LB film suggests the LB film structure is the same as those solid-state calcium alkylphosphonates containing long-chain alkyl groups.

Polarized ATR-FTIR was used to establish the tilt angles of the octadecylphosphonate molecules in the divalent metal phosphonate LB films. The tilt angle of IR-active vibrational modes within layered organic films can be determined from the ratio of IR absorbances measured in two polarization directions.[33,99,100] The absorbance of the $\nu_a(CH_2)$ band was recorded with s- and p-polarized light for each film, and the resulting tilts of the alkyl chain with respect to the normal of the metal ion plane are given in Table 2-3. Since the LB films are each comprised of octadecylphosphonate bilayers, their layer thickness should be similar, with differences arising from variations in the tilting of the alkyl chains. The less the alkyl chains tilt from the normal, the larger the layer thickness.

The alkyl chain tilt angles, determined by polarized FTIR, are similar for each of the films and are consistent with the layer thicknesses measured by X-ray diffraction.

Extended Lattice Structure

Typically, inorganic ions in LB films such as metal carboxylate films serve to add stability to the transferred film by crosslinking and holding together the organic portion of the film. Although the ionic interactions between the polar headgroup and the metal ion in metal carboxylate LB films determine the structure of the transferred film, little attention has been devoted to using ionic headgroup interactions to purposefully control monolayer structure. Zasadzinski performed AFM studies on a series of divalent metal carboxylate LB films which revealed that the structures of the organic films were dependent upon the nature of the metal ion/headgroup interaction.[32] In these materials, the alkyl chains vary their packing, tilt angle, and tilt direction to achieve close-packing in the film, but it is the metal ion/headgroup lattice energy that dictates the molecular area.

Many investigations have been carried out to determine the structure of solid-state divalent metal organophosphonates. Syntheses of divalent metal phosphonates by varying the metal ions as well as the organic groups has lead to the conclusion that the structure of these hybrid organic/inorganic materials is directed by the choice of metal ion. In 1979, Cunningham *et al.* deduced that the metal ions in the series $M(O_3PC_6H_5)\cdot H_2O$ (M = Mg, Mn, Co, Cu, Ni) have an octahedral coordination but were unable to carry out X-ray structure determinations.[19] Several years later, crystals of $Mn(O_3PC_6H_5)\cdot H_2O$ were grown and an X-ray structure refined in the orthorhombic space group $Pmn2_1$ was reported.[15] In 1990, a thorough structural study on two series of divalent metal phosphonates, $M(O_3PR)\cdot H_2O$ (M = Mg, Mn, Zn, Ca, Co, Cd; R=n-alkyl, aryl group) and $M(HO_3PR)_2$ (M = Ca) was completed.[13] For M=Mg, Mn, Co, Zn in the first series, the phosphonates crystallize in the orthorhombic layered structure of $Mn(O_3PC_6H_5)\cdot H_2O$, with interlayer distances to accomodate the different R groups. For M=Ca or Cd in the

same series, a structure of lower symmetry is adopted. For calcium, the larger ionic radius is expected to be the reason for the difference.[13] In the second series, calcium forms 1:2 salts with alkylphosphonates having alkyl groups containing five carbon atoms or greater. Cao et al.[16] determined that cadmium forms 1:1 salts with phosphonic acids crystallizing in the orthorhombic space group, $Pna2_1$ with cadmium ions octahedrally coordinated by five phosphonate oxygen atoms and a water molecule. The only difference in structure between the cadmium, manganese and magnesium phosphonates is that the MO_6 octahedron in manganese and magnesium methylphosphonates possesses a mirror symmetry whereas the CdO_6 octahedron in cadmium alkylphosphonates does not.[16] The stacking of the layers along the a axis in $Cd(O_3PCH_3)\cdot H_2O$, for example, are different from the stacking of the layers in manganese and magnesium organophosphonates.[16] In the latter, the layers are translationally related along the b axis whereas in $Cd(O_3PCH_3)\cdot H_2O$ the layers are related by an a-glide plane perpendicular to the b axis. The a-glide causes the layers to repeat in every other layer along the a axis, resulting in an a-axis dimension twice of the interlayer distance.[16] In all solid-state transition metal phosphonates it is, therefore, the inorganic lattice energy that dictates the observed layered structures regardless of the organic group. The differences between the cadmium, manganese, cobalt, magnesium and calcium structures is attributed to more ionic bonding within the inorganic lattice in the calcium solids and more covalent bonding in the metal lattices in the other solids.

We have taken advantage of these ionic headgroup interactions to purposefully control monolayer structure and have shown that the inorganic lattice in the LB films can be used to dictate the structure of the LB film. The extended lattice structures are formed during the deposition process. The metal phosphonate "precipitates" upon draining of water from the film as the substrate is withdrawn from the subphase. Since the source of organophosphonic acid is restricted to the pre-arranged Langmuir monolayers, the metal phosphonate "crystallization" is controlled by the deposition procedure. The deposition is limited to a single layer at a time, and the metal phosphonate layers grow exclusively

parallel to the substrate. XPS data indicate that the $M(O_3PR)\cdot H_2O$ films are all fully ionized. In the FTIR, the PO_3^{2-} stretching modes are very sensitive to the mode of phosphonate binding,[13,101] and in the LB films they are as well resolved as they are in the solids, indicating that the metal phosphonate binding is uniform throughout the film. There is no evidence for large areas of amorphous metal-phosphonate structure.

Summary

When comparing the structural characterization of the different LB films, it can be concluded that each divalent metal phosphonate LB film forms with an extended lattice metal phosphonate network. The metal phosphonate bonding in each case is understood by comparing the LB films to known metal phosphonate solids, and each film adopts a known solid-state layered structure. The in-plane layered structure is determined by optimizing the metal-phosphonate binding. Although the organic groups are the same in each case, even the metal to phosphonate ratios can be changed by choice of divalent metal. This is dramatically illustrated by the different structures seen for the Cd^{2+} and Ca^{2+} films where the ionic radii are expected to be similar.[13,16] Such differences are well known in solid-state chemistry, but are not as widely considered when evaluating LB film structure, although the importance of the metal/headgroup interaction has recently been pointed-out in structural studies of a series of metal carboxylate LB films.[32] We have fabricated, layer-by-layer, high quality single-layer analogs of known solid-state structures via a wet chemical method. Previously the preparation of single layers of an inorganic solid was only achieved by dry processes including chemical vapor deposition, physical vapor deposition, ion beam deposition or electrochemical methods.[102-104] These methods are limited to substrates whose surface structure is suitably matched to the depositing layer, and controlling molecular orientations is very difficult.[103] As a consequence of the extended lattice structures, properties normally associated soley with inorganic compounds

can now be incorporated with ease into organic films using the Langmuir-Blodgett technique.

CHAPTER 3
AN ELECTRON PARAMAGNETIC RESONANCE STUDY OF A LANGMUIR-BLODGETT FILM OF MANGANESE OCTADECYLPHOSPHONATE AND COMPARISON OF THE MAGNETIC PROPERTIES TO SOLID-STATE MANGANESE ALKYLPHOSPHONATES

Introduction

The layered nature of many solid-state metal phosphonates has attracted attention from researchers with a variety of interests. Solid-state structural studies have revealed several new layered structures for different combinations of metal ion and organophosphonate group.[13,14,16,18,105-108] The large internal surface areas in the solids, that result from the layered structures, suggest potential applications as catalyst supports and sorbents, and in sensing and separation applications.[16,20,22,109] The metal-phosphonate binding interaction has also been used in procedures to deposit monolayer and multilayer thin films.[21,26-30,110-114] The process deposits layers of functionalized organic molecules by alternately exposing a surface to solutions of metal ions and α,ω-disubstituted organophosphonic acids, and has been used to prepare thin films for applications that require oriented assemblies of organic molecules.[28,29,110,111] In yet another area of interest, some of the transition metal phosphonates have been the subject of magnetic studies where the layered structures give rise to unusual magnetic properties and serve as useful models for investigating magnetic behavior in two-dimensional systems.[57,58,115]

Manganese organophosphonates crystallize in the orthorhombic space group $Pmn2_1$. The crystal structure of $Mn(O_3PC_6H_5)\cdot H_2O$ reported by Cao et al.[15] nicely shows the layered nature of the solids and a view of the manganese phosphonate plane is reproduced in Figure 3-1.[15] The structure consists of layers of manganese ions, which are

Figure 3-1. Structure of manganese phenylphosphonate, $Mn(O_3PC_6H_5)\cdot H_2O$ viewed down the **b** (stacking) axis. Phenyl groups were omitted for clarity. The powdered manganese alkylphosphonates are isostructural with the phenylphosphonate shown here. Structural data were taken from reference 15. (Cross-hatched circles - Mn; large dotted circles - P; small open circles - O).

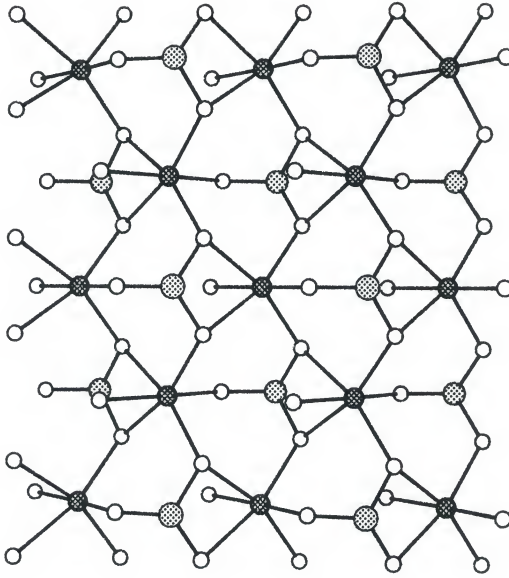

roughly co-planar, octahedrally coordinated by five phosphonate oxygens and one water of hydration. The phenyl groups are pointed away from the inorganic layer, approximately perpendicular to the manganese ion plane, and make van der Waals contacts between layers. The manganese alkyl phosphonates, $Mn(O_3PC_nH_{2n+1})\cdot H_2O$, have the same in-plane structure as the phenyl analog and the interlayer spacing varies as the alkyl group is changed.[15,57] Unit cell parameters for some manganese alkylphosphonates are given in Table 3-1.

Table 3-1. Structural and Magnetic Parameters for $Mn(O_3PR)\cdot H_2O$ Solids[(a)]

Compound	a, Å	b, Å	c, Å	-J/k, K
$Mn(O_3PCH_3)\cdot H_2O$	5.82	8.82	4.90	2.70
$Mn(O_3PC_2H_5)\cdot H_2O$	5.83	10.24	4.87	2.78
$Mn(O_3PC_3H_7)\cdot H_2O$	5.84	11.71	4.91	2.48
$Mn(O_3PC_4H_9)\cdot H_2O$	5.84	14.72	4.91	2.48

(a) Reference 23[57]

Carling et al.[57] have performed static susceptibility measurements on powder samples of a series of manganese alkylphosphonates, $Mn(O_3PC_nH_{2n+1})\cdot H_2O$ (n = 1-4). The susceptibility as a function of temperature for each sample is characteristic of antiferromagnetic exchange in a low-dimensional lattice, and values of the nearest neighbor exchange, J, determined by Carling et al. from fitting the data to a model for a two-dimensional Heisenberg antiferromagnet, are listed in Table 3-1.[57] The exchange constant, J, is defined according to the Hamiltonian, $H = -J\Sigma S_i S_j$, and a value of $J < 0$ indicates antiferromagnetic exchange. Each of the materials orders antiferromagnetically with ordering temperatures in the range 14.8-15.1 K.[57] Below the Néel temperature, T_N,

the presence of a weak magnetic moment indicates that these materials are best described as canted antiferromagnets, which are also called "weak ferromagnets."[57]

In the last chapter, it was demonstrated that inorganic extended-lattice monolayers of a variety of the metal phosphonates could be prepared using Langmuir-Blodgett film deposition methods.[76,77] In the case of manganese octadecylphosphonate, it was shown using X-ray diffraction, XPS and FTIR that the LB film has the same structure that is observed in several of the solid-state manganese alkylphosphonates.[76] In this chapter, a detailed EPR study of the manganese octadecylphosphonate LB film is presented, and the magnetic behavior of the LB film is compared to published magnetism studies on the series of solid-state manganese alkylphosphonates.[57] It will be demonstrated that properties such as magnetic exchange inherent to the inorganic lattice can be incorporated into organic Langmuir-Blodgett films.

EPR experiments on low-dimensional systems provide detailed information about spin dynamics in magnetically exchange-coupled systems.[116,117] In this chapter it will be demonstrated from the EPR results, that the LB film of manganese octadecylphosphonate is well described as a two-dimensional manganese lattice with nearest-neighbor Heisenberg antiferromagnetic exchange, and the magnitude of the exchange is the same as observed in the solids. The EPR behavior confirms that the manganese phosphonate LB film contains an inorganic extended-lattice structure.

Experimental Section

Materials

Octadecylphosphonic acid, $C_{18}H_{37}PO_3H_2$, was used as purchased from Alfa chemicals (Ward Hill, MA). Manganese chloride tetrahydrate, $MnCl_2{\cdot}4H_2O$, was used as purchased from Fisher Scientific (Orlando, FL).

Instrumentation

Langmuir-Blodgett films were prepared using a KSV (Stratford, CT) 3000 Langmuir-Blodgett trough modified to operate with double barriers. Purified water having a resistivity of 18 MΩ-cm was used. EPR spectra were recorded on a Bruker (Billerica, MA) ER 200D spectrometer modified with a digital signal channel and a digital field controller. Data were collected using a U.S. EPR (Clarksville, MD) SPEC300 data acquisition program and analyzed using a U.S. EPR EPRDAP data analysis program. Temperature was controlled using an Oxford Instruments (Witney, England) ITC 503 Temperature Controller and ESR 900 cryostat.

Procedure

Manganese octadecylphosphonate LB films were prepared by spreading octadecylphosphonic acid onto an aqueous subphase containing 5×10^{-4} M $MnCl_2 \cdot 4H_2O$ held in a pH range of 5.2-5.6. The monolayer was compressed to a pressure of 17 mN/m and bilayers were transferred onto a 625 mm^2 calcium arachidate covered mylar substrate at speeds of 8 mm/min on the downstroke and 5 mm/min on the upstroke. Multilayers cannot be formed by continuous deposition of the film due to cross-linking of the phosphonate groups by the manganese ions at the air/water interface. After deposition of a bilayer, the monolayer was removed from the surface of the trough and a new octadecylphosphonic acid monolayer was formed. Films containing 50 bilayers were prepared and transfer ratios were in the range 0.98-1.08.

Samples for EPR studies were deposited onto mylar sheets. After film deposition, the mylar was cut into thin strips that were stacked and placed in a conventional EPR tube. The oriented sample could then be rotated with respect to the magnetic field, as shown in Figure 3-2. The LB film sample has a common interlayer or **b** axis, all the layers are parallel to the substrate, but because the film is composed of ordered domains the in-plane

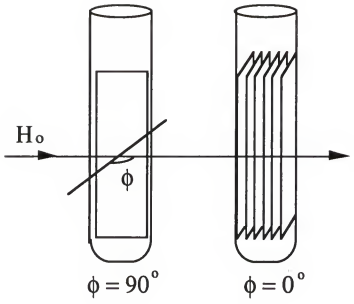

Figure 3-2. Orientations with respect to the magnetic field, H_o, of the LB film stacked in a conventional EPR tube.

orientation (**ac** plane) is circularly averaged. The angle ϕ is defined as the angle between the film normal and the direction of the static field, as illustrated in Figure 3-2.

Results and Discussion

Representative EPR signals of the LB film are shown in Figure 3-3. At high temperatures the shape of the EPR line is mainly dominated by two factors, dipolar interactions and exchange interactions.[116] Dipolar interactions between paramagnetic centers tend to broaden the EPR lines, while exchange interactions tend to narrow lines.[116] In low-dimensional materials the exchange interaction is less effective than in three-dimensional materials because the number of spins which are exchange coupled to a given spin is less than in the three-dimensional case.[116] The signals for both the LB film and the solid-state samples are dipolar broadened as expected for a lattice of manganese ions, and no Mn^{2+} hyperfine splitting is observed. The g-values are characteristic of Mn^{2+} in a

Figure 3-3. EPR spectra of the manganese octadecylphosphonate LB film at 250 K, 50 K, and 20 K. The sample was oriented with $\phi = 0^{\circ}$ (Figure 3-2). The EPR signal broadens substantially as the temperature is lowered below 30 K.

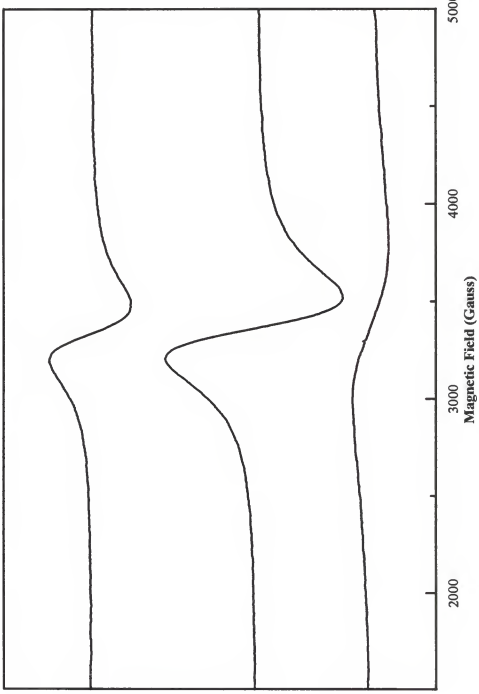
2000
3000
4000
5000
Magnetic Field (Gauss)

nearly cubic field and are consistent with the g-value of 1.99 observed for a powder sample of $Mn(O_3PC_3H_7)\cdot H_2O$. In contrast to the powdered solid-state samples, the LB films have a common b-axis orientation and the g values vary continuously as the sample is rotated with respect to the external field, although the values are nearly isotropic ranging from 1.99 to 2.00.

The room temperature EPR linewidth of the LB film is plotted as a function of sample orientation in Figure 3-4. Spectra were taken as the sample was rotated every five degrees with respect to the magnetic field. The shape of the plot is consistent with the behavior predicted for a two-dimensional lattice with antiferromagnetic Heisenberg exchange.[60,116,118-120] In contrast to a three-dimensional material where the linewidth decreases according to $(\cos^2\phi - 1)$ as the sample is rotated from 0° to 90°, in low-dimensional materials, the contribution to the linewidth originating from spin diffusion has a $(3\cos^2\phi - 1)^n$ dependence where n = 4/3 for a one-dimensional lattice and n = 2 for a two-dimensional lattice.[116,118-120] The expected orientational dependence of the linewidth for a two-dimensional Heisenberg antiferromagnet is, therefore,

$$\Delta H = A + B(3\cos^2\phi - 1)^2 \qquad (3\text{-}1)$$

where A and B encompass exchange and other dipolar interaction terms.[116,119,120] A fit of the data with A = 218 G and B = 20 G is superimposed on the data in Figure 3-4. The linewidth has a minimum of 218 G at the magic angle $\phi = 54.7°$ where the secular contribution of spin diffusion vanishes.[116]

The integrated area of the EPR signal is proportional to the spin susceptibility, and a plot of 1/area vs. temperature is shown in Figure 3-5. An extrapolation of the high temperature data intercepts the temperature axis at -34 K indicating nearest neighbor antiferromagnetic exchange. The data are also expressed in Figure 3-6 as area vs. temperature with the solid line being a fit to the data. The area of the EPR signal gradually increases as the temperature is lowered and reaches a maximum near 25 K. The area then decreases rapidly until the EPR signal is lost around 17 K. The shape of the plot is

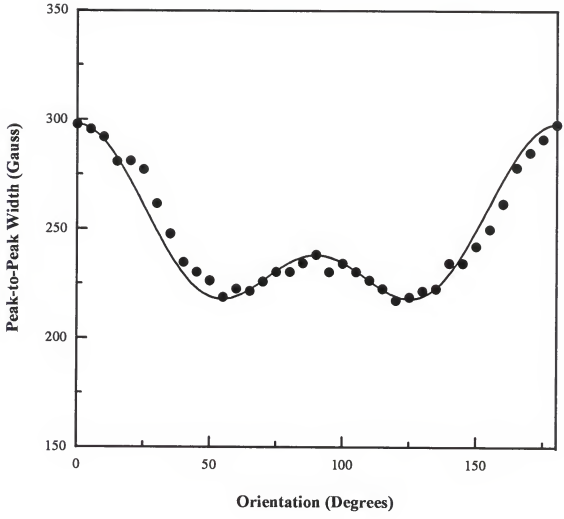

Figure 3-4. EPR linewidth as a function of sample orientation at room temperature. The sample orientation is defined in Figure 3-2. The solid line is a fit to $\Delta H = A + B(3\cos^2\phi - 1)^2$ with A = 218 G and B = 20 G. The behavior is characteristic of a two-dimensional lattice with antiferromagnetic Heisenberg exchange.

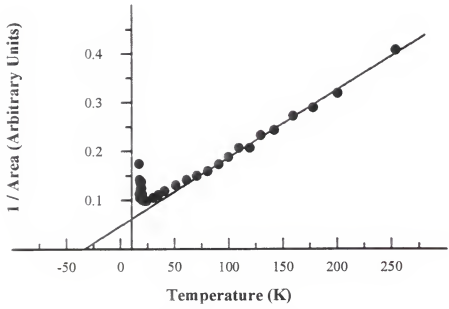

Figure 3-5. Temperature dependence of the inverse of the area (arbitrary units) of the EPR signal from the manganese octadecylphosphonate LB film. The solid line is a linear fit to the data above 80 K. An extrapolation of the high temperature data intercepts the temperature axis at -34 K, indicating antiferromagnetic exchange.

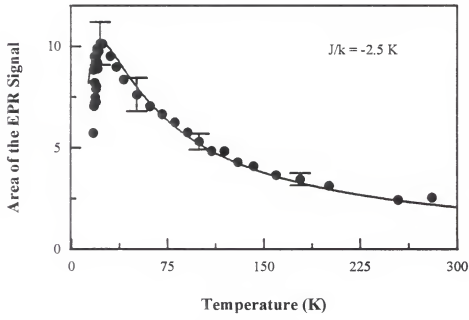

Figure 3-6. Temperature dependence of the integrated area (arbitrary units) of the EPR signal from the manganese octadecylphosphonate LB film. The solid line is a fit to the data using equation 2 for a two-dimensional lattice with Heisenberg antiferromagnetic exchange with exchange constant J/k = -2.8 K. Since the EPR intensity is plotted as arbitrary units, the fit has been fixed to the EPR intensity at 110 K.

characteristic of antiferromagnetic exchange in a low-dimensional solid,[60,118,121,122] and the behavior is nearly identical to the temperature dependent static susceptibility of the powdered solid-state manganese alkylphosphonates.[57]

Although there is no exact solution for the magnetic susceptibility χ, of a quadratic-layer Heisenberg antiferromagnet, the temperature dependence can be described by a numerical series expansion[122]

$$Ng^2\mu_B^2/\chi = 3\theta + \Sigma(C_n/\theta^{n-1}) \qquad (3\text{-}2)$$

where $\theta = kT/JS(S+1)$, g is the Lande factor, N is the number of spins, μ_B is the Bohr magneton, and J is the nearest neighbor exchange constant. The coefficients, C_n, for S = 5/2 have been calculated up to n = 6 by Lines.[121] The value of the exchange constant can be estimated by the temperature of maximum susceptibility, T_{max}, according to $kT_{max}/J = 2.06S(S+1)$.[123] Taking T_{max} as 25 K yields J/k = -2.8 K and a fit to the data according to equation 2 is plotted as the solid line in Figure 3-6. Because the EPR intensity is plotted as arbitrary units, the fit has been fixed to the EPR intensity at 110 K. The value of the exchange constant, J/k = -2.8 K, agrees closely with the exchange constants for the bulk metal alkylphosphonates obtained by Carling et al.[57] and shown in Table 3-1. The fit of the EPR intensity to the numerical expression in equation 3-2 is further evidence that the LB film is a two-dimensional antiferromagnetic exchange-coupled lattice. The magnitude of the exchange is nearly identical to the solid-state analogs and suggests that the in-plane Mn-O-Mn interactions in the film are similar to those seen in the solid state-structures.

The peak-to-peak widths of the EPR signals of the manganese octadecylphosphonate LB film and a powder sample of manganese propylphosphonate are plotted as a function of temperature in Figure 3-7. In both cases the EPR linewidth remains approximately constant as the temperature is lowered below room temperature. As the temperature approaches 30 K, the linewidths broaden rapidly until the signals become so broad they are lost below 17 K. The powder sample undergoes a magnetic ordering transition at $T_N = 14.90$ K to a canted antiferromagnetic state.[57] The increase in linewidth

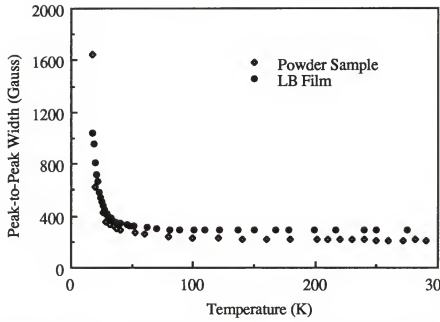

Figure 3-7. EPR linewidth as a function of temperature for a powder sample of manganese propylphosphonate and for the manganese octadecylphosphonate LB film. The rapid increase in linewidths seen below 30 K is characteristic of systems approaching a magnetic ordering transition.

is characteristic of a system approaching a magnetic ordering transition and is caused by antiferromagnetic fluctuations. Large variations in the local field, caused by regions of short range order fluctuating to achieve long range order, result in the large linewidths. The LB film also experiences antiferromagnetic fluctuations, although by EPR we cannot observe whether or not an ordering transition occurs because the signal becomes too broad and vanishes at the temperature of the anticipated transition.

Magnetic ordering is not predicted to occur in a truly two-dimensional Heisenberg lattice.[52,53,124] When ordering is observed in layered systems it occurs as a result of either anisotropy in the exchange or a dimensionality crossover in a temperature regime where the interlayer exchange, $J_{\perp}$, becomes important.[1,58,118] It is interesting to note that in the series $Mn(O_3PC_nH_{2n+1})\cdot H_2O$, where ordering does occur, dimensionality crossover has been observed to occur at values of the reduced temperature, $(T_N - T)/T_N$, of 0.085, 0.015,

and 0.010 for n = 2, 3, 4, respectively.[58] For the LB films, interlayer exchange is not expected as the interlayer spacing is 48.5 Å. Also, as a result of the depositon process, layers are not in registry. The LB films should behave as isolated monolayers and dimensionality crossover should not occur.

The EPR behavior of the manganese phosphonate LB films can be compared to previous studies of magnetic exchange between metal ions in LB films. The most extensive studies are those of Pomerantz et al.[34,60,125,126] on LB films of manganese stearate. Based on linewidth analyses and temperature dependent EPR intensity data, antiferromagnetic exchange was also observed in the manganese stearate LB film and the value of the nearest-neighbor exchange was estimated as $J/k = -1.0 \pm 0.4$ K.[125] This value is smaller than the -2.8 K value for the manganese phosphonates and is related to differences in the in-plane structure of the two films. In the metal phosphonate film, in-plane bonding is well described by the structures of the known solid-state analogs. The manganese ions are nearly co-planar and each site is coordinated by five phosphonate oxygens and one water molecule. Adjacent manganese ions are bridged by a single phosphonate oxygen which mediates magnetic superexchange. The structure of the manganese stearate films is less clear.[34] The Mn^{2+} ions are certainly bridged by the carboxylate headgroups, but the mode of binding is not known. TED and AFM studies suggest a rectangular arrangement of Mn^{2+} ions.[32]

The observation of large shifts in resonance field at low temperatures was cited as evidence for spontaneous magnetization in the manganese stearate films.[127] Since the exchange is predominantly antiferromagnetic, the magnetic moment was attributed to canting of the antiferromagnetically ordered spins. However, direct observation of the ordered state has not been observed. An alternative explanation offered by Pomerantz[127] for the increased magnetization is the possibility of an antiferromagnetic lattice containing manganese ion vacancies, which cannot be discounted considering the LB film deposition method. The only evidence for ordering in the manganese phosphonate films is the large

increase in linewidth at low temperature. As was discussed above, this is a precursor effect and is not itself evidence for ordering, although, the similarities in the behavior of the LB film and the powdered solids where ordering does occur are striking. It will be informative to study the magnetization of these films to lower temperature, but because of the limited sample size, the use of standard methods for measuring the static susceptibility have not yet been possible. In the next chapter however, a method of characterization was developed so magnetic susceptibility of the LB films at at low temperatures, down to 5 K, could be measured. The results of the magnetic investigations will be discussed in detail in the next chapter.

Summary

EPR studies of manganese octadecylphoshonate Langmuir-Blodgett films reveal that the magnetic exchange in the films is identical to that exhibited in solid-state manganese alkylphosphonates. The high temperature magnetic behavior, above T_N of the powders, for both the film and the solid-state materials is characteristic of antiferromagnetic Heisenberg exchange in a two-dimensional lattice. At room temperature, the angular dependence of the EPR linewidth is characteristic of a two-dimensional lattice of manganese spins. Temperature dependent behavior of the manganese LB film indicates the manganese Heisenberg spins undergo nearest neighbor antiferromagnetic exchange in a two-dimensional lattice. The value of the antiferromagnetic exchange constant of the manganese octadecylphosphonate LB film is comparable to the values of the antiferromagnetic exchange constants for the structurally analogous manganese alkylphosphonate powders. While the solid-state manganese alkylphosphonates order to form "weak ferromagnets", direct observation of a transition to long-range order is not possible in the LB films using EPR. However, the EPR linewidth at low temperature is characteristic of a system approaching a magnetic ordering transition. Magnetization

measurements are needed below 17 K to explore the ground state of the two-dimensional LB film.

The magnetic studies help confirm that the LB film has the same extended lattice structure as the solid-state alkylphosphonates. These results demonstrate that single layers of known solid-state layered structures can be prepared using LB methods. Since the inorganic lattice energy is the dominant interaction in the metal phosphonate layered structures, the possibility exists of using these structures to organize LB films of organophosphonates containing organic groups other than alkyl chains, in analogy to the known solid-state metal phosphonates based on functional organic groups.

CHAPTER 4
A MAGNETIC LANGMUIR-BLODGETT FILM

Introduction

Known for most of this century, the Langmuir-Blodgett (LB) method is perhaps the earliest technique to afford molecular level control over the dimensions of supramolecular assemblies.[43] The LB technique organizes amphiphilic molecules into a close-packed monolayer, at a water surface, which is then transferred to a solid support that is pushed or pulled through the film at the air/water interface.[33,42,72] Many fundamental areas of research have made use of this ability to arrange molecules and control the chemistry of interfaces, including studies of membrane dynamics,[72] biomineralization at organic interfaces,[128] and electron and energy transfer processes in controlled geometries,[78] while some practical applications of LB films include use in organic-based electronic devices,[129] organic non-linear optical devices,[130,131] and chemical and biochemical sensors.[72] However, many potential applications have not been realized because of the metastable nature of the layered organic assemblies, and in particular, the demonstration of physical properties that require long-range structural order, such as superconductivity or magnetic order, has been elusive. In this dissertation thus far the approach to developing long-range two-dimensional structural order in LB films is to utilize the inorganic lattice energy of known solid-state layered structures and incorporate inorganic extended lattice structures into the hydrophilic portion of Langmuir-Blodgett assemblies.[76,77] In addition to adding structural order to the film, this approach provides the opportunity to introduce physical properties normally associated with inorganic extended lattice structures. As a demonstration of this concept, the characterization of a magnetic LB film will be presented in this chapter. Manganese octadecylphosphonate LB films undergo a transition to long

range magnetic order and below the ordering temperature exhibit a spontaneous magnetization characteristic of a "weak ferromagnet." These results are the first demonstration of cooperative ordering phenomena in LB films.

There are several examples of mixed organic/inorganic layered compounds where polar ionic networks are separated by nonpolar organic networks,[9] and the LB films studied here are modeled after one such class of materials, the family of solid-state layered transition metal phosphonates.[17,21,64] Figure 4-1 shows the crystal packing diagram for manganese phenylphosphonate using the crystal coordinates given by Cao et al.[15] In manganese phenylphosphonate and other manganese phosphonates containing straight chain alkyl groups, metal ions are crosslinked by the phosphonate groups which bind both above and below the metal ion plane.[15] The metal ions are coordinated by five oxygens from four different phosphonate groups and the distorted octahedral coordination is completed by a water of hydration. Layers are held together by van der Waals interactions between the organic groups in adjacent layers. The distance between manganese planes in succesive layers depends on the sizes of the organic groups.

The magnetic properties of a series of manganese alkylphosphonates $Mn(O_3PC_nH_{2n+1})\cdot H_2O$, n = 1-4, have been investigated by Carling et al,[57,58] and these authors have shown that at high temperatures the manganese phosphonates behave as two-dimensional Heisenberg antiferromagnets and that at lower temperatures (14.8 - 15.1 K) each member of the series undergoes a magnetic ordering transition. The ordered state has a spontaneous magnetization due to incomplete cancellation of the antiferromagnetically coupled moments. Such systems are known as canted antiferromagnets or "weak ferromagnets". The manganese octadecylphosphonate films described in this chapter are LB analogs of the solid-state manganese phosphonates, possessing structural and magnetic properties that are comparable to the solids.

Figure 4-1. Structure of $Mn(O_3PC_6H_5)\cdot H_2O$ viewed down the **a** axis. Crystallographic data taken from reference15. (Cross-hatched circles - Mn; large dotted circles - P; small open circles - O).

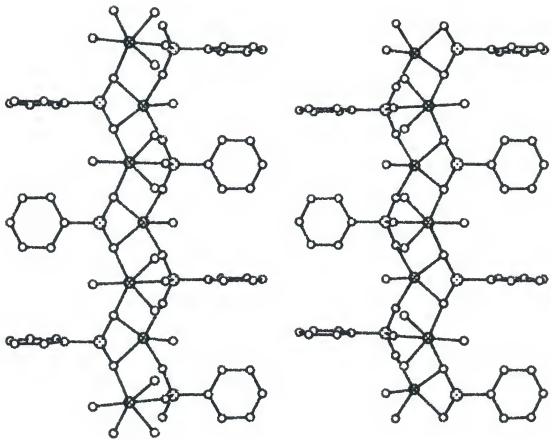

Experimental Section

Materials

Octadecylphosphonic Acid, $CH_3(CH_2)_{17}P(O)(OH)_2$, 98% was purchased from Alfa Aesar chemicals (Ward Hill, MA). Manganese chloride tetrahydrate and calcium chloride were used as purchased from Fisher Scientific (Fair Lawn, NJ). Arachidic Acid, $C_{19}H_{39}COOH$, was used with no further purification as purchased from Aldrich Chemicals. Mylar sheets, purchased from Dupont, were sonicated in ethanol for 20 minutes prior to use.

Instrumentation

Langmuir-Blodgett films were prepared using a KSV (Stratford, CT) 3000 Langmuir-Blodgett trough modified to operate with double barriers. Purified water having a resistivity of 18 MΩ-cm was used. Magnetization experiments were performed using a Quantum Design MPMS SQUID magnetometer. A gelcap and plastic straw were used as a sample holder during the measurements. The background signals arising from the gelcap and straw were measured independently and subtracted from the raw data.

Procedure

Manganese octadecylphosphonate bilayers were prepared using conventional LB deposition techniques.[76] Octadecylphosphonic acid was spread on an aqueous subphase containing 5×10^{-4} M $MnCl_2 \cdot 4H_2O$ and held in a pH range of 5.2-5.6. The monolayer was compressed to a surface pressure of 17 mN/m and bilayers, one layer on the downstroke and one layer on the upstroke, were deposited onto hydrophobic substrates. For the magnetic measurements, an 81 bilayer film was deposited onto both sides of a calcium arachidate covered mylar sheet having a total area of 5.5 cm^2 and resulting in a

sample of 6 x 10^{-7} mol which was then cut up into small pieces, 3mm x 3mm. The mylar pieces were stacked and oriented in a gelcap which was held in the magnetometer with a plastic straw.

Results and Discussion

Structure and High Temperature Magnetic Behavior of Manganese Octadecylphosphonate Langmuir-Blodgett Films

As discussed in the two previous chapters and as a brief review, the deposited manganese films are layered and several orders of the (00*l*) Bragg peak are observed in X-ray diffraction, corresponding to an interlayer separation of 48.5Å. A 1:1 manganese phosphorus ratio in the films was confirmed by XPS. In the ATR-FTIR spectra, the shapes and energy of the C-H stretching bands are consistent with an organized array of all-trans alkyl chains, and the P-O stretching modes confirm that the metal-phosphonate binding interactions in the LB film are the same as those in the solids. Magnetic exchange in the LB film was demonstrated as a result of the EPR study[79] showed that the magnitude of the nearest-neighbor exchange, J/k_B = -2.8K, is nearly identical to the values found by Carling et al.[57,58] for the solid-state manganese phosphonates. At temperatures below 50K, the EPR line width begins to increase and becomes too broad to measure below 17K. This behavior is consistent with antiferromagnetic fluctuations, a precursor to magnetic ordering, but no direct observation of the ordered state is seen in the EPR.

Magnetic Behavior of the Manganese LB Film at Low Temperatures (5 K - 25 K)

An ordering transition was observed in the static magnetization measurements of manganese octadecylphosphonate LB films. For the magnetic measurements, the background contribution of the gelcap and straw was measured independently and subtracted from the data. The temperature dependent magnetization of the LB film, measured upon warming the film between 5K and 25K and recorded with the measuring

field of 0.01T parallel to the plane of the film, is shown in Figure 4-2A for the cases where the sample was cooled from room temperature in zero applied field (ZFC) and where the sample was cooled in a magnetic field of 0.1 T (FC). The ZFC data show the signature of an ordering transition at 13.5 K. The FC data also show the ordering transition, and the increased magnetization below the ordering temperature (T_N) is evidence for spontaneous magnetization of the film. The spontaneous magnetization is shown more clearly in Figure 4-2B, where the difference between the FC and ZFC magnetization (ΔM) is plotted. While the mass of the sample is small compared to the sample holder and mylar substrate, the difference plot subtracts the signal due to the sample support and allows quantification of the film magnetization. Below T_N, the magnetization increases and begins to level off as the temperature approaches 5K. The magnitude of the magnetization is calculated from the magnetic data of the film measured in the parallel orientation. Using the equation, $M = N(\mu_{ferro}/\mu_B)\mu_B$[132] where N = Avogadro's number, μ_B = the Bohr magneton, and taking M = 44.5 emu/mol from the data, the moment at 5K corresponds to a ferromagnetic moment of $\mu_{ferro}/\mu_B = 8 \times 10^{-3}$. The weak moment in the ordered state is consistent with antiferromagnetic ordering of the lattice where coupled nearest neighbor moments do not exactly cancel due to low site symmetry giving rise to a "weak ferromagnetic" state. The magnitude of the ferromagnetic moment is similar to the moments observed for the manganese alkylphosphonate solid-state analogs.[57] A canting angle of the spins in the manganese LB film is also determined from the magnetic data. For an isotropic (g=2) S=5/2 spin, the effective ferromagnetic moment, $\mu_{eff} = g[S(S + 1)]^{1/2}\mu_B = 5.92$.[132] A canting angle α, is calculated using $\alpha = \sin^{-1}(\mu_{ferro}/\mu_{eff})$. In the manganese LB films, a canting angle of 0.1° is observed. This angle is similar to the angles observed in the powdered manganese alkylphosphonate samples.[57]

Field dependent magnetization data obtained at 2K at applied fields up to 5T are shown in Figure 4-3 for two orientations of the film. When a system is in the

Figure. 4-2. Magnetization *vs.* temperature for an 81 bilayer film with the measuring field applied parallel to the plane of the film. **(A)** Comparison of the data taken upon warming the film after cooling in zero applied field (ZFC) and cooling in a field of 0.1T (FC). In both cases the measuring field is 0.01T. The ordering transition (T_N) is seen as the discontinuity in the ZFC plot at 13.5K. **(B)** The difference of the two plots in (A) showing the spontaneous magnetization below T_N.

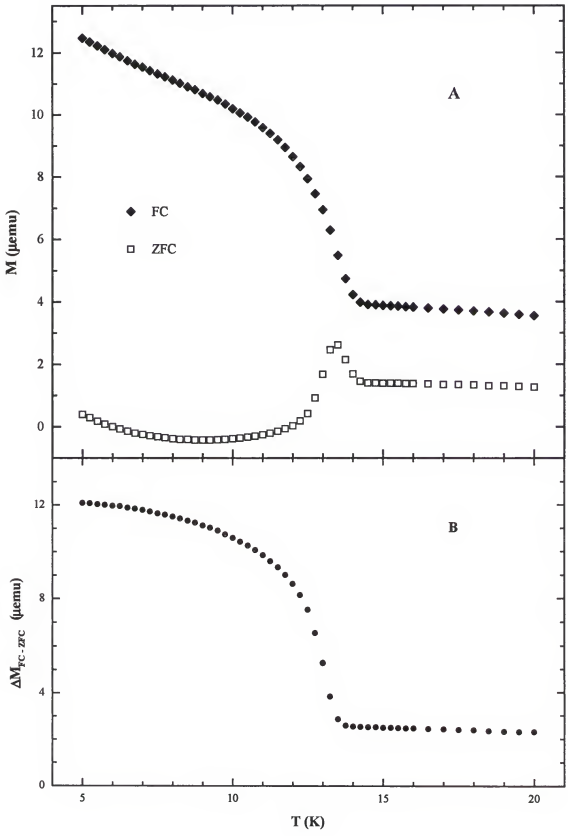
A
B
FC
ZFC
M (μemu)
ΔM_{FC-ZFC} (μemu)
T (K)
0
2
4
6
8
10
12
5
10
15
20

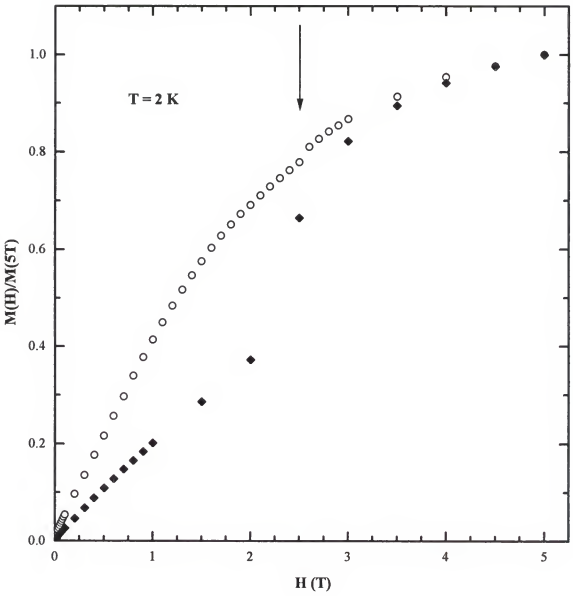

Figure. 4-3. Magnetization *vs.* applied field at 2K, normalized to the value at 5T, with the applied field directed perpendicular (filled diamonds) and parallel (open circles) to the plane of the film. The spin flop transition is seen in the perpendicular orientation at 2.5T. A small inflection is seen in the parallel orientation due to imperfect alignment of the individual mylar sheets with respect to the field.

antiferromagnetic state, $T < T_N$, and the field is applied parallel to the easy axis, a phase transition known as a spin flop transition can occur.[132] At the critical field value, known as the spin flop field, the moments flop perpendicular to the field.[132] At this point, a discontinuity in the magnetization is observed. For the case where the applied field is oriented perpendicular to the plane of the film, shown as the filled diamonds in Figure 4-3, there is evidence for a spin-flop transition at $H_{app} = 2.5T$. The spin-flop transition in this orientation indicates that the axis of antiferromagnetic alignment is perpendicular to the plane of the film and therefore perpendicular to the manganese phosphonate layers. This type of arrangement is shown schematically in Figure 4-4. While the magnetic structures of the solid-state organophosphonates have not yet been determined, the magnetic structure of a purely inorganic isomorph, $KMnPO_4{\cdot}H_2O$, is known from magnetic scattering in its neutron diffraction profile[133] The structure shows that the manganese moments are antiferromagnetically coupled within the manganese phosphate planes and aligned perpendicular to the planes, which is consistent with the behavior observed for the LB film.

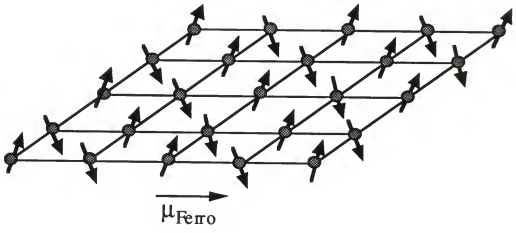

Figure 4-4. Illustration of the orientation of the manganese spins in manganese organophosphonates. Each manganese moment is canted with respect to the two-dimensional plane. Antiferromagnetic coupling between nearest neighbor moments results in a net magnetic moment along the two-dimensional plane of manganese ions.

Canting of the antiferromagnetically coupled moments therefore puts the "weak ferromagnetic" moment in the manganese phosphonate plane, or parallel to the plane of the film. This is also observed in $KMnPO_4 \cdot H_2O$, where the canting is in-plane toward the crystallographic c-axis.[133] With the field oriented parallel to the plane of the LB film, the magnetization gradually increases with increasing applied field (open circles shown in Figure 4-3) as is expected if the antiferromagnetic hard axis lies in the plane. There is a small inflection corresponding to the spin-flop transition, seen at $H_{app} = 2.5T$, which is due to imperfect alignment of the sample with respect to the external field.

The LB film also exhibits magnetic memory below T_N. Figure 4-5 plots magnetization in the vicinity of zero field, for positive and negative scans of the applied field as it is cycled between $\pm$ 5T. Hysteresis is the signature of magnetic memory, and a small coercive field of 20mT and remnant magnetization of 10 μemu are seen. Although the effect is small, the result demonstrates that the LB method can be used to produce thin magnetic films, and as far as we are aware, this work represents the first observation of magnetic order in an LB film. Magnetic studies of LB films are mostly limited to EPR analysis of organic radicals or metal complexes in transferred films. While evidence for magnetic exchange between molecular species in LB films has been observed in some instances,[134,135] there are no examples of magnetically ordered molecular films. The most extensive investigations of magnetism in LB films have focused on manganese stearate[34,126] where precursor effects to antiferromagnetic ordering were seen in the EPR line width and g-value at temperatures approaching 2K, but no ordering transition has been observed. The enhanced magnetic exchange in the manganese phosphonate films is due to superexchange *via* the phosphonate ligand, and the extended lattice structure of the film provides sufficient structural order for magnetic ordering to take place.

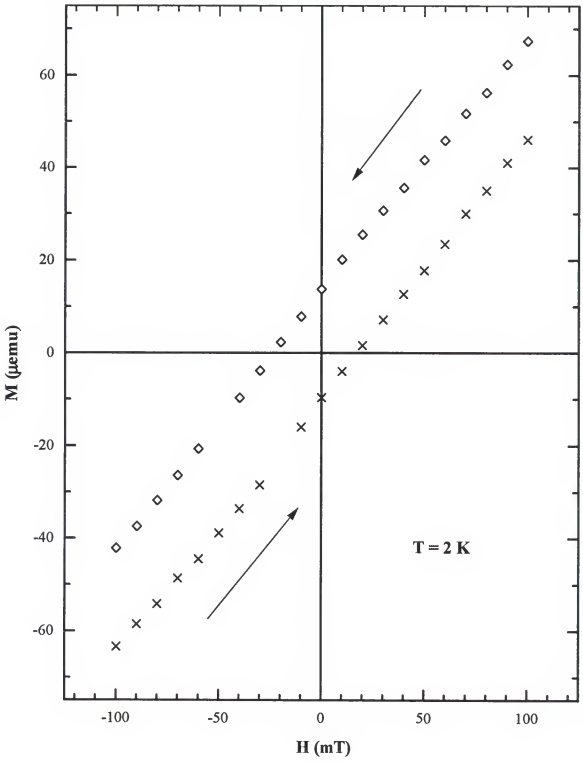

Figure 4-5. Magnetization at 2K in the vicinity of zero field showing hysteresis during cycling between ±5T. The applied field is oriented perpendicular to the plane of the film. A remnant magnetization of 10 μemu and a coercive field of 20 mT are observed.

CHAPTER 5
MAGNETIC CHARACTERIZATION OF ALTERNATING MANGANESE/CADMIUM PHOSPHONATE LANGMUIR-BLODGETT FILMS

Introduction

The fabrication of materials at a molecular level continues to be a topic of interest among many chemists. The ability to control and tune intermolecular interactions within thin films and surfaces has enormous potential for many applications such as catalysis, sensing, separations, and information storage. Attempts at molecular architecture, by means of the layer-by-layer deposition of alternating metals onto solid substrates, have been carried out using dry chemical methods such as chemical vapor deposition and molecular beam epitaxy.[136-139] While the preparation of alternating layers of inorganic/inorganic and organic/inorganic solids is achieved using these techniques, these methods are somewhat restricted to substrates whose surface structure is suitably matched to the depositing layer. In previous chapters, it is shown that the Langmuir-Blodgett technique is a wet chemical method that can be used for the layer-by-layer deposition of high-quality, extended-lattice, organic/inorganic layered structures.

The prospect of molecular control over the properties of LB films, initiated the construction of organic/inorganic LB films containing alternating layers of different metals within the inorganic portion of the films. This chapter discusses attempts at preparing LB films containing alternating layers of cadmium and manganese octadecylphosphonate. Characterization of LB films of this nature cannot be achieved using many of the methods described in chapter two because the properties of the two different types of layers often interfere. Therefore, characterization of the alternating manganese/cadmium LB films involves the exclusive use of X-ray photoelectron spectroscopy and magnetization

experiments. Utilization of these two techniques is possible since the properties of the manganese and cadmium ions can be measured without interference.

Before interpreting the magnetic behavior of a manganese octadecylphosphonate LB film containing cadmium octadecylphosphonate between the manganese layers, one must recall that a magnetic transition to long range order, and the temperature at which the transition occurs, in a two-dimensional layered Heisenberg material depends on the structural and magnetic construction of the compound. Since a transition to long range magnetic order is forbidden for a 2-dimensional Heisenberg system, if a magnetic transition occurs, a crossover in either lattice dimensionality or spin dimensionality must also occur.[1] When the magnetic interactions between consecutive layers in a quasi 2-dimensional solid become larger than the in-plane magnetic interactions, characteristic 3-dimensional ordering is observed.[1] The temperature at which ordering occurs depends upon the size of the interlayer magnetic exchange. The weaker the interlayer exchange interactions, the lower the ordering temperature.[132] For the case of the manganese octadecylphosphonate LB film, the separation between consecutive manganese layers is quite large and any interlayer interactions should be negligible. The insertion of cadmium octadecylphosphonate between manganese phosphonate layers should not change the ordering temperature significantly relative to the pure manganese phosphonate film, assuming no interlayer mixing of the metals.

When the in-plane magnetic correlation length is sufficiently larger than the interlayer interactions, if a transition to long range magnetic order is observed, a crossover from Heisenberg, or three-dimensional spin, to Ising, one-dimensional spin accompanies the transition.[1] In pure manganese organophosphonate Langmuir-Blodgett films, it is speculated that the observed transition to long range spontaneous magnetism must be due to a crossover in spin dimensionality. In alternating manganese/cadmium octadecylphosphonate LB films, assuming that cadmium and magnanese ions are confined

to their separate consecutive layers, the magnetic behavior of manganese films is not anticipated to change.

However, if cadmium and manganese ions mix within the inorganic layers, the magnetic behavior should change since the in-plane structure of the manganese lattice would be modified. If ion exchange occurs, a small percentage of cadmium is incorporated within the manganese layers, and the result is a diluted antiferromagnetic LB film. Non-magnetic impurities in magnetic layers are known to cause decreases in the ordering temperature, relative to the pure compound. Previous reports have demonstrated that the magnetic properties of several two-dimensional solids change upon dilution of the magnetic species.[55,140-142] Relative to the pure materials, magnetically diluted, quasi two-dimensional, layered solids have resulted in depressions of the ordering temperature at relatively low dopant levels, to complete elimination of the ordering transition at higher dopant levels.[1,55,140] The value of the critical concentration of magnetic ions at which ordering is totally suppressed depends on the lattice dimensionality, the magnetic coordination number and also on spin-dimensionality.[1]

Experimental Section

Materials

All chemicals were purchased and used without further purification. Octadecylphosphonic Acid, $CH_3(CH_2)_{17}P(O)(OH)_2$, 98% was purchased from Alfa Aesar chemicals (Ward Hill, MA). Manganese chloride tetrahydrate, $MnCl_2{\cdot}4H_2O$, and $CaCl_2$ (97.8%) were purchased from Fisher Scientific (Fair Lawn, NJ). Cadmium chloride hemihydrate, $CdCl_2{\cdot}2.5H_2O$, and arachidic acid, $C_{19}H_{39}COOH$, were obtained from Aldrich Chemicals (Milwaukee, Wisconsin). Mylar sheets were purchased from Dupont. Octadecyltrichlorosilane (OTS, $C_{18}H_{37}SiCl_3$, 95%) was purchased from Aldrich and

stored under N_2. A Barnstead Nanopure (Boston, MA) purification system produced water with an average resistivity of 18 MΩ-cm for all experiments.

Instrumentation

Langmuir-Blodgett films were prepared using a KSV (Stratford, CT) 3000 Langmuir-Blodgett trough modified to operate with double barriers. Purified water having a resistivity of 18 MΩ-cm was used.

Magnetization experiments were performed using a Quantum Design MPMS SQUID magnetometer. A gelcap and plastic straw were used as a sample holder during the measurements. The background signals arising from the gelcap and straw were measured independently and subtracted from the raw data.

X-ray photoelectron spectra were obtained using a Perkin-Elmer (Eden Prairie, MN) PHI 5000 Series spectrometer. All spectra were taken using the Mg K_α line source at 1253.6 eV. The spectrometer has a typical resolution of 2.0 eV, with anode voltage and power settings of 15 kV and 300 W, respectively. Typical operating pressure was 5×10^{-9} atm. Survey scans were performed at a 45° take-off angle with a pass energy of 89.45 eV. Multiplex scans, 140 scans over each peak, were run over a 20 eV range with a pass energy of 35.75 eV. The observed relative intensities were determined from experimental peak areas normalized with atomic and instrument sensitivity factors.[84,85]

Substrate Preparation

Single crystal (100) silicon wafers, purchased from Semiconductor Processing Company (Boston, MA), were used as deposition substrates for the XPS measurements. The silicon substrates were cleaned using the RCA cleaning procedure[82] then dried under N_2. Octadecyltrichlorosilane (OTS) was self-assembled[39,83] onto the silicon wafers to make them hydrophobic by placing the wafers in a 2% solution of OTS in hexadecane for

30 minutes. The wafers were then rinsed with chloroform to remove any excess hexadecane, and dried under a stream of nitrogen.

For the magnetic measurements mylar sheets were the substrates. The mylar sheets were sonicated in ethanol for 30 minutes and made hydrophobic by depositing ten bilayers of calcium arachidate onto the mylar using standard Langmuir-Blodgett procedures. Arachidic acid was spread onto an aqueous subphase containing 5×10^{-4} M $CaCl_2$ at a pH of 6.5. The monolayer was compressed to a pressure of 27 mN/m. Bilayers of calcium arachidate were transferred at speeds of 10 mm/min on both the upstroke and downstroke. Bilayers of alternating manganese and cadmium octadecylphosphonate or manganese/cadmium octadecylphosphonate mixed films were then deposited onto the calcium arachidate covered mylar substrates.

Preparation of Alternating Manganese/Cadmium Octadecylphosphonate LB Films

Two types of Langmuir-Blodgett films of alternating manganese and cadmium octadecylphosphonate were prepared and are illustrated in Figure 5-1. Type I films consisted of bilayers of manganese octadecylphosphonate separated by one bilayer of cadmium octadecylphosphonate, and type II films comprised bilayers of manganese octadecylphosphonate separated by two bilayers of cadmium octadecylphosphonate. LB films of alternating manganese and cadmium octadecylphosphonate were prepared using conventional LB deposition techniques.[76] The procedure for the type I alternating films involved spreading octadecylphosphonic acid onto an aqueous subphase containing 5×10^{-4} M $MnCl_2 \cdot 4H_2O$ held in a pH range of 5.2-5.6. The monolayer was compressed to a surface pressure of 17 mN/m and one layer on the downstroke and one layer on the upstroke, was deposited onto a hydrophobic substrate at rates of 8 mm/min and 5 mm/min, respectively. After the complete transfer of one bilayer of manganese octadecylphosphonate, the Mn^{2+} subphase was drained from the trough and the trough was rinsed twice with nanopure water. The LB trough was then filled with a subphase

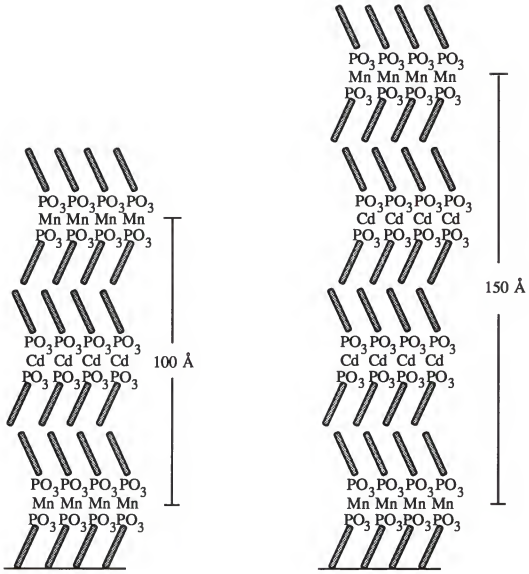

Figure 5-1. Illustration of Two Types of Alternating Manganese/Cadmium Octadecylphosphonate LB films.

containing 5 x 10^{-4} M $CdCl_2 \cdot 2.5H_2O$ held at a pH of approximately 5. Octadecylphosphonic acid was spread on this Cd^{2+} containing subphase and a new monolayer was compressed to a surface pressure of 20 mN/m. One layer of the film was transferred onto the substrate on the downstroke at a rate of 8 mm/min and the bilayer was completed by transferring one layer on the upstroke at a rate of 5 mm/min. The trough was again drained, rinsed twice with nanopure water, and refilled with the manganese subphase. For the magnetic measurements, the entire procedure was repeated until 81 bilayers of manganese octadecylphosphonate were transferred onto a mylar substrate having a total area of 12.47 cm^2 and resulting in a sample consisting of 8.42 x 10^{17} manganese ions. The mylar was then cut up and oriented into a gel cap for magnetic measurements.

The procedure for forming type II alternating manganese/cadmium films was identical to that of type I, except, instead of transferring only one bilayer of cadmium octadecylphosphonate, two bilayers of cadmium octadecylphosphonate were transferred onto the substrate before cleaning the trough and replacing with the manganese subphase. In all cases, transfer ratios of about one were acquired. The sample used for the magnetization measurements contained 50 bilayers of manganese octadecylphosphonate on a total substrate area of 15.6 cm^2. The resulting sample consisted of 6.5 x 10^{17} manganese spins.

Preparation of Mixed Manganese/Cadmium Octadecylphosphonate LB Films

Mixed manganese/cadmium octadecylphosphonate LB films were prepared by spreading octadecylphosphonic acid onto a subphase containing various amounts of both manganese and cadmium chloride held at a pH of about 5. The monolayer was compressed to a surface pressure of 17 mN/m and transferred onto substrates at rates of 8 mm/min on the downstroke and 5 mm/min on the upstroke. Transfer ratios of approximately one were obtained.

Results and Discussion

X-ray photoelectron spectroscopy is used to determine if the metal ions in LB films of alternating manganese and cadmium octadecylphosphonate exchange between metal layers or if the metals remain in each layer without any interchange. Figure 5-2 shows the integrated XPS signals from manganese, cadmium and phosphorus from two different alternating manganese/cadmium LB film samples. The observed relative areas are compared to the expected intensities. The XPS sample in Figure 5-2A of a type I LB film consists of one bilayer of manganese octadecylphosphonate transferred onto a hydrophobic silicon wafer with the next bilayer being cadmium octadecylphosphonate. The XPS spectrum of a second sample fabricated in reverse when compared to the first sample is shown in Figure 5-2B. In this type I LB film, cadmium octadecylphosphonate was first deposited onto a hydrophobic silicon wafer and the second bilayer comprised manganese octadecylphosphonate.

The calculated relative intensities for the manganese, cadmium and phosphorus signals were obtained using the layered model described in detail in chapter two. For the calculations, the inelastic mean free path of the manganese electrons is, $\lambda_{e,Mn}$ = 26.9 Å for phosphorus, $\lambda_{e,P}$ = 36.8 Å and for the cadmium electrons, $\lambda_{e,Cd}$ = 31.9 Å. In the first sample where the cadmium layer is closer to the surface, an overlayer thickness for cadmium is estimated to be d_{Cd} = 24.3 Å and for manganese, d_{Mn} = 74.4 Å. In the second sample, values for the manganese and cadmium overlayer thicknesses were estimated as 24.3 Å and 74.4 Å, respectively. In both calculations of the expected relative intensities, overlayer thicknesses for phosphorus were estimated as 22.5 Å, 26.1 Å, 72.6 Å, and 76.2 Å. Within experimental error of the XPS spectrometer, ±3%, close agreement between experimentally observed intensities and calculated intensities are reported, however small percentages of metal ion exchange cannot be disregarded.

Figure 5-3 plots magnetization (FC-ZFC) as a function of temperature for a type I manganese octadecylphosphonate LB film containing 81 bilayers of manganese with each

Figure 5-2. Integrated areas of the manganese, cadmium, and phosphorus XPS signals of two alternating manganese/cadmium phosphonate LB films. (A) XPS spectrum from a two bilayer sample in which the top bilayer is cadmium octadecylphosphonate and the bottom layer is manganese octadecylphosphonate. (B) XPS spectrum of a two bilayer sample where manganese octadecylphosphonate is the top layer and cadmium octadecylphosphonate is the bottom layer. The observed relative intensities of each peak are compared with the expected percentages. Calculation of the relative intensities are explained in the text.

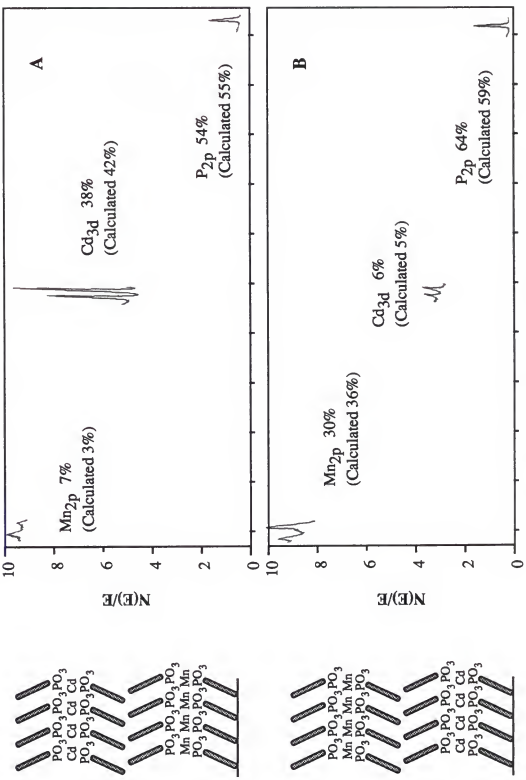
A
Mn2p 7%
(Calculated 3%)
Cd3d 38%
(Calculated 42%)
P2p 54%
(Calculated 55%)
B
Mn2p 30%
(Calculated 36%)
Cd3d 6%
(Calculated 5%)
P2p 64%
(Calculated 59%)
N(E)/E
Binding Energy (eV)
PO3 PO3 PO3 PO3
Cd Cd Cd Cd
PO3 PO3 PO3 PO3
Mn Mn Mn Mn
PO3 PO3 PO3 PO3

Figure. 5-3. Magnetization vs. temperature for a type I 81 bilayer film of manganese octadecylphosphonate with each manganese layer separated by one bilayer of cadmium octadecylphosphonate. The measuring field is applied parallel to the plane of the film. The difference in the magnetization data taken upon warming the film after cooling in zero applied field (ZFC) and cooling in a field of 0.1T (FC) shows a spontaneous magnetization below the ordering transition (T_N) of 10.5 K. In both cases the measuring field is 0.01T.

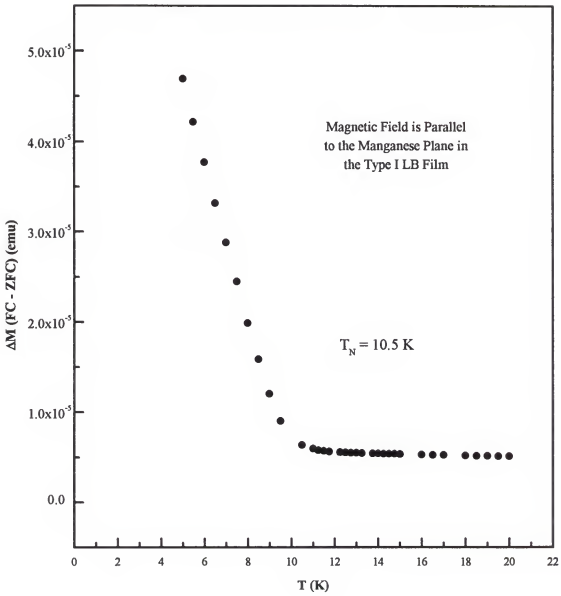
Magnetic Field is Parallel
to the Manganese Plane in
the Type I LB Film
T_N = 10.5 K
ΔM (FC - ZFC) (emu)
T (K)
5.0x10⁻⁵
4.0x10⁻⁵
3.0x10⁻⁵
2.0x10⁻⁵
1.0x10⁻⁵
0.0
0
2
4
6
8
10
12
14
16
18
20
22

manganese layer separated by one bilayer of cadmium octadecylphosphonate. A transition to long range order is observed at about 10.5 K. Figure 5-4 shows magnetization as a function of field for the same sample oriented with the magnetic field perpendicular to the plane of the LB film. The anticipated spin flop transition which was observed in the pure manganese LB film is now masked, and small inflections or changes in slope of the magnetization are observed at approximately 2 T and 3.25 T.

Figure 5-5 and 5-6 are the magnetization (FC - ZFC) vs. temperature and magnetization vs. magnetic field plots for a type II LB film consisting of 50 bilayers of manganese octadecylphosphonate with each manganese layer separated by two bilayers of cadmium octadecylphosphonate, respectively. As in the previous sample, a ferromagnetic moment is observed below 10.5 K in the magnetization vs. temperature plot. Measuring the magnetization of the sample as a function of magnetic field yields no spin flop transition, and again only a small inflection of the magnetization is noted just above 2 T.

In both cases, magnetization experiments reveal a depression of the ordering temperature of the expanded manganese LB films, relative to the pure manganese LB film. It is well understood[1,55] that in any two-dimensional material, decreases in the interlayer magnetic exchange, and the presence of nonmagnetic impurities present in the magnetic layers tend to suppress the temperature at which long range order occurs. Pure manganese octadecylphosphonate LB films are described as truly two-dimensional materials exhibiting spontaneous magnetization below 13.5 K due solely to the intralayer interactions of canted manganese spins. Interlayer interactions are not expected in pure manganese LB films and, therefore, interlayer interactions are not expected in alternating manganese/cadmium LB films. Thus, a transition to long range order is expected to occur at the same temperature. The resulting decrease of the ordering transition temperature in the alternating manganese/cadmium films is, therefore, attributed to cadmium impurities in the manganese layers. Small amounts of nonmagnetic impurities disrupt the makeup of the intralayer

Figure. 5-4. Magnetization vs. applied field at 2K for the type I manganese LB Film. The spin flop transition which was observed in the perpendicular orientation at 2.5 T for the pure manganese LB film is now masked by nonmagnetic cadmium impurities. A small inflection is observed at 3.25 T.

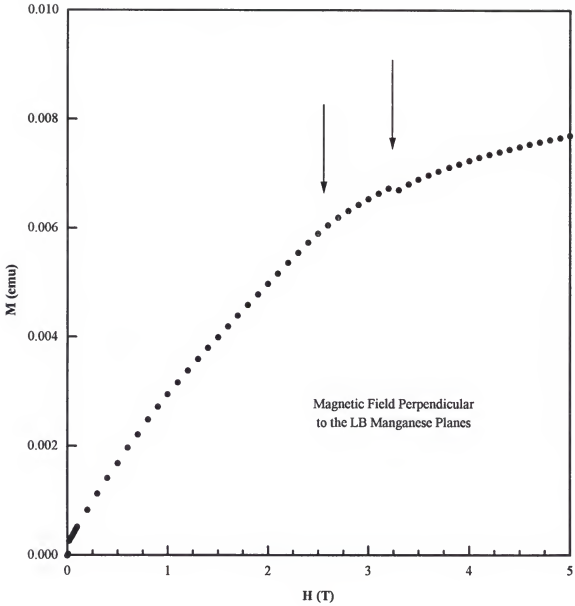
0.010
0.008
0.006
0.004
0.002
0.000
M (emu)
0
1
2
3
4
5
H (T)
Magnetic Field Perpendicular
to the LB Manganese Planes

Figure. 5-5. Magnetization vs. temperature for a type II manganese octadecylphosphonate LB film with the measuring field applied parallel to the plane of the film. To be consistent with the previous magnetic measurements performed on the type I films, the difference in the magnetization data were taken upon warming the film after cooling in zero applied field (ZFC) and cooling in a field of 0.1T (FC) using a measuring field is 0.01T. The results shows a spontaneous magnetization below the ordering transition of 10.5 K.

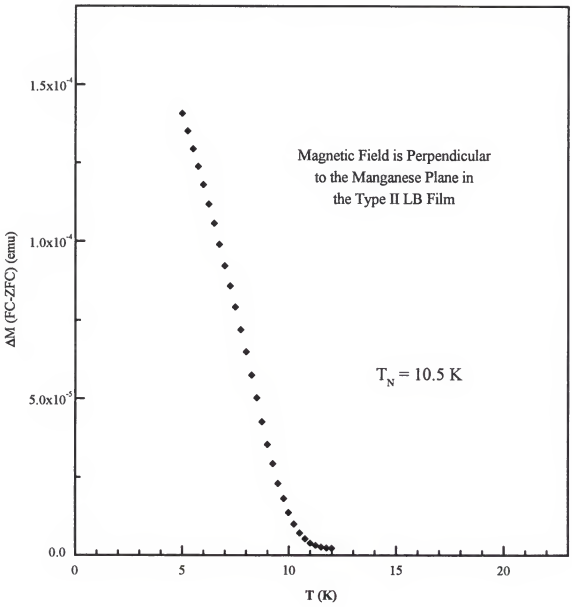
Magnetic Field is Perpendicular
to the Manganese Plane in
the Type II LB Film
T_N = 10.5 K
ΔM (FC-ZFC) (emu)
1.5x10^{-4}
1.0x10^{-4}
5.0x10^{-5}
0.0
0
5
10
15
20
T (K)

Figure. 5-6. Magnetization *vs*. applied field at 2K for the type II manganese LB film. The spin flop transition is once again masked by nonmagnetic impurities and only a small inflection is observed.

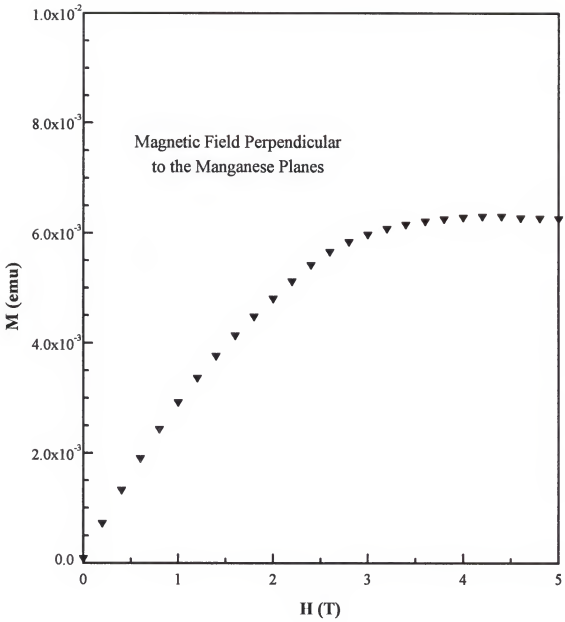
Magnetic Field Perpendicular
to the Manganese Planes
M (emu)
H (T)
1.0x10-2
8.0x10-3
6.0x10-3
4.0x10-3
2.0x10-3
0.0
0
1
2
3
4
5

magnetic moments and the sample must be cooled to lower temperatures in order to achieve an ordered state.

Magnetic measurements provide an excellent method to characterize and understand the magnetic structure of the manganese-containing Langmuir-Blodgett films. Orientational magnetization measurements performed on pure manganese films, reveal that the manganese moments are antiferromagnetically exchange coupled along the axis perpendicular to the manganese layers. Since the moments are canted, a weak ferromagnetic moment lies along the plane of the manganese ions, perpendicular to the easy axis, as illustrated in Figure 5-7A. Any observed magnetization measured in the direction parallel to the easy axis is small, and is a result of misalignment of the mylar strips in the gel cap. On the contrary, magnetic measurements performed on alternating manganese/cadmium LB samples reveal larger ferromagnetic moments when the samples are aligned perpendicular to the magnetic field of the spectrometer. The enhanced magnetization for the alternating manganese/cadmium samples can be attributed to uncompensated manganese spins. If small amounts of cadmium ions are incorporated into the manganese layers, magnetically, this could result in an odd number of exchange coupled manganese spins, referred to as uncompensated spins, as depicted in Figure 5-7B. The result for such a sample is a moment, parallel to the easy axis of the film.

A quantitive estimate of the uncompensated manganese moments can be arrived at using two different methods. In the first method, calculation of the percent uncompensated spins is determined by comparing the magnetization measurements of the alternating manganese/cadmium samples with the magnetization measurements of the pure manganese LB film. Calculation of the number of uncompensated manganese spins will be explained using the type I LB film as an example. At saturation, 2 K and 5 T, the difference in the magnetization between the type I film and the pure manganese film when the magnetic field is applied perpendicular to the manganese planes, is 1.77×10^3 emu/mol. This difference

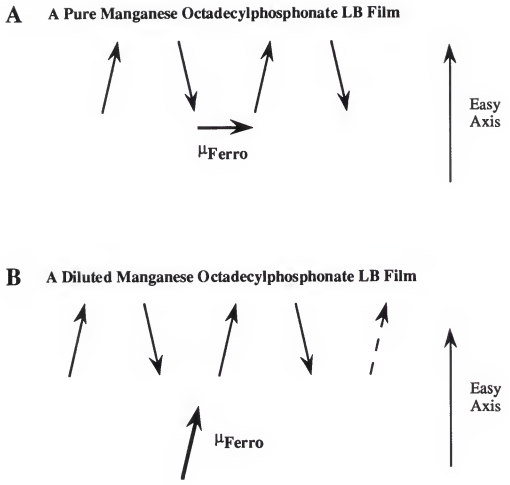

Figure 5-7. Illustration of the orientation of manganese moments in manganese octadecylphosphonate LB films. (A) Antiferromagnetic exchange of canted manganese moments in the pure manganese phosphonate film results in a net ferromagnetic moment perpendicular to the easy axis of the film. (B) Antiferromagnetic exchange of the canted manganese moments in dilute manganese LB films results in some uncompensated moments, as indicated by the dashed arrow. The result is a net ferromagnetic moment parallel, or nearly parallel to the easy axis of the film.

is the magnetization due to uncompensated manganese spins in the type I LB film. Using equation 5-1 the number of uncompensated spins may be determined.[132]

$$M = Ng\mu_B S \qquad (5\text{-}1)$$

Assigning values M = [(1.77 x 10^3 emu/mol)*(1.4 x 10^{-6} mol)], g = 2, μ_B = 0.927 x 10^{-20} erg/G, and S = 5/2 the number of uncompensated spins, N is 5.3 x 10^{16}. Since there are a total of 8.4 x 10^{17} manganese spins in the type I LB film, the amount of uncompensated spins corresponds to 6%. After a similar calculation on the type II film, the amount of uncompensated manganese spins is expected to be about 7%.

An estimate of the percent uncompensated spins in the manganese layers can also be determined when the observed changes in ordering temperatures are compared with similar results dealing with magnetic investigations on diluted antiferromagnets cited in the literature.[1,140,141] The magnetic behavior of a variety of diluted, layered antiferromagnets and ferromagnets, such as $K_2Mn_pMg_{1-p}F_4$, $K_2Co_pMg_{1-p}F_4$ and $La_2Cu_{0.95}Li_{0.05}O_4$, where p represents the amount of magnetic material in the diluted magnet, have been reported.[1,55,140] In all cases, a depression of the ordering temperature is noted. For the $K_2Mn_pMg_{1-p}F_4$ compounds, which approximate the manganese LB films most closely, as the amount of magnesium is increased, the transition to long range order decreases until p reaches about 0.6. At a 40% nonmagnetic impurity level, no long range order is observed and the sample behaves as a simple Curie magnet. The change in the ordering transition in the diluted antiferromagnet is described using equation 5-2.[1,55,140]

$$T_N(p) = \{T_N(1)\}[1 - d(1 - p)] \qquad (5\text{-}2)$$

In the above equation, p represents the amount of magnetic material in the diluted antiferromagnet, $T_N(p)$ is the ordering temperature of the diluted antiferromagnet, $T_N(1)$ is the ordering temperature of the sample containing no nonmagnetic impurities, and d is an empirical constant adjusted to fit to the experimental data. For two-dimensional materials, d = 3.5. Using 10.5 K as the transition temperature of the diluted AF LB film, $T_N(p)$, and

13.5 K as the transition temperature for the pure manganese LB film, $T_N(1)$, a value of p = 0.94 is obtained.

The magnetization vs. field experiments on the type I and type II LB films, Figures 5-4 and 5-6, show no prominent discontinuities in the data as observed in the pure manganese LB film. In the pure manganese octadecylphosphonate LB film, the discontinuity of the magnetization at 2.5 T corresponds to the spin flop field. These features are not expected to be observed in the type I and II films if cadmium is present in the manganese layers. Previous reports on diluted antiferromagnets such as $K_2Mn_pMg_{1-p}F_4$, have resulted in similar behavior.[140] The presence of the nonmagnetic impurities tends to mask the observation of the spin flop field.[140] Thus it can be explained that the cadmium impurities in the manganese/cadmium alternating films act to conceal the spin flop transition.

The magnetic behavior of the so-called alternating manganese/cadmium LB films provide a very useful method for the structural characterization of the films. Since the results suggest that a small percentage of cadmium ions are exchanging with manganese ions in the films, LB films of mixed manganese and cadmium octadecylphosphonate were prepared to determine if the magnetic behavior of these films exhibit characteristics similar to the alternating manganese/cadmium films. In the mixed LB films, manganese and cadmium ions are added together in various percentages in the same subphase. It was expected that manganese and cadmium would be randomly distributed throughout the inorganic portion of the transferred octadecylphosphonate LB film. The formation of the first mixed manganese/cadmium film involved preparing a subphase containing 85% Mn^{2+} and 15% Cd^{2+} held at a pH of about 5. X-ray photoelectron spectroscopy was used to determine precisely the quantity of each metal contained in the organic film. Figure 5-8A is the XPS spectrum of a three bilayer sample of a cadmium/manganese mixed film. The integrated relative intensities of the manganese and cadmium signals indicate that the LB film actually contains about 34% cadmium and 66% manganese. Magnetization

Figure. 5-8. XPS and magnetization experiments on mixed manganese/cadmium octadecylphosphonate LB films containing 34% cadmium. (A) XPS spectrum of a three bilayer mixed manganese/cadmium LB film. Integrated relative intensities of the manganese, cadmium and phosphorus signals indicate there is 34% cadmium present in the manganese layers. (B) Magnetization vs. applied field at 2K for the 34% cadmium containing manganese film. The magnetic field is aligned parallel to the plane of the LB film. The sample is characteristic of a Curie paramagnet and the curve can be fit to 4 x 10^{17} spins acting independently, as shown by the solid line.

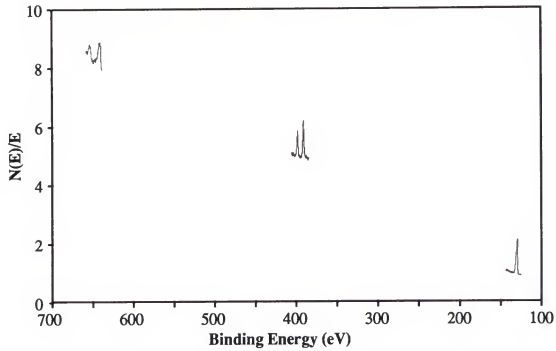
N(E)/E
Binding Energy (eV)
0
2
4
6
8
10
700
600
500
400
300
200
100

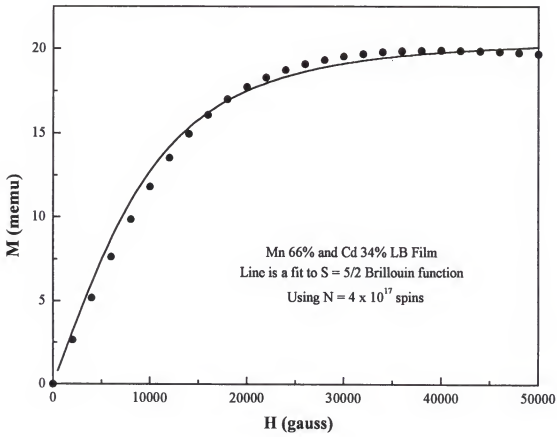
M (memu)
H (gauss)
Mn 66% and Cd 34% LB Film
Line is a fit to S = 5/2 Brillouin function
Using N = 4 x 10^17 spins
0
5
10
15
20
0
10000
20000
30000
40000
50000

measurements of a sample prepared under identical conditions, were performed on a 75 bilayer film transferred onto a piece of mylar having an area of 9.6 cm^2. With 66% of the ions in this sample being manganese, the number of manganese moments in the sample is about 6×10^{17}. Magnetization as a function of magnetic field is plotted in Figure 5-8B for the 34% cadmium/ 66% manganese octadecylphosphonate LB film. At this high percentage of nonmagnetic doping, the sample exhibits Curie-like behavior. The magnetization data can be fit nicely to a Brillouin function using 4×10^{17} spins. The fit is shown by the solid line in Figure 5-8B.

Magnetization measurements were also performed on an LB film comprising 12% cadmium and 88% manganese in the inorganic layers. This time, the film was formed on a LB trough consisting of an aqueous subphase of 95% Mn^{2+} and 5% Cd^{2+} held at a pH of 5. The percentages of metal incorporated in the film were again determined using XPS and the integrated intensities of the manganese, cadmium, and phosphorus peaks are displayed in Figure 5-9A. As in the previous sample, cadmium binds more strongly to the phosphonate head groups and is incorporated at a percentage higher than anticipated. Magnetic experiments on a phosphonate LB film containing 12% cadmium and 88% manganese is shown in Figure 5-9B. As in the previous sample, it is found that 12% cadmium in the manganese layers is too high and a transition to long range order is not observed. The data are fit to a Brillouin function using 5×10^{17} magnetic moments, as shown by the solid line in Figure 5-9B. In this film, the manganese spins act independently and paramagnetic behavior is observed, therefore indicating the cadmium ion impurity level is too high to observe antiferromagnetic exchange between the manganese moments.

Summary

Magnetic susceptibility measurements were performed on manganese octadecylphosphonate LB films containing layers of cadmium octadecylphosphonate. The

Figure. 5-9. XPS and magnetization behavior of a mixed manganese/cadmium octadecylphosphonate LB films containing 12% cadmium. (A) XPS spectrum of a three bilayer mixed manganese/cadmium LB film. Integrated relative intensities of the manganese, cadmium and phosphorus signals indicate there is 12% cadmium present in the film. (B) Magnetization vs. applied field for the 12% cadmium containing film. The magnetic field is aligned parallel to the plane of the LB film and held at a temperature of 2 K. The sample behaves as a paramagnet and the curve can be fit to a Brillioun function using 7.6×10^{17} spins as shown by the solid line.

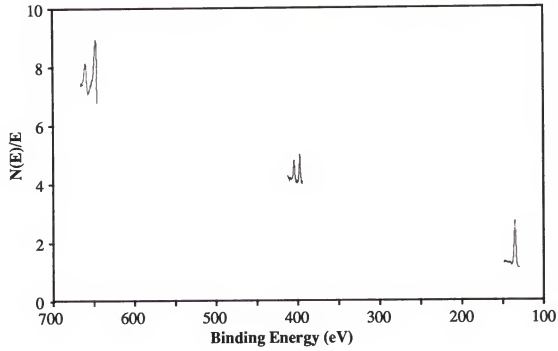
N(E)/E
Binding Energy (eV)
10
8
6
4
2
0
700
600
500
400
300
200
100

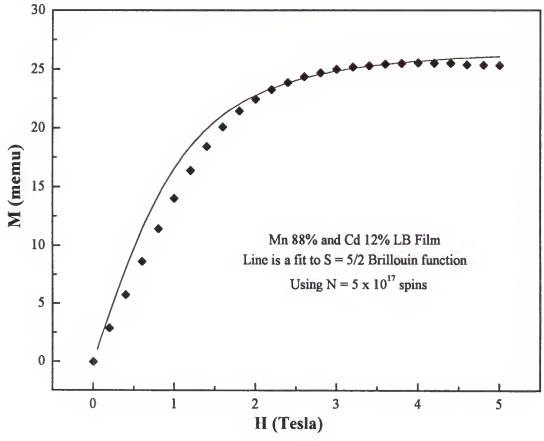
M (memu)
H (Tesla)
Mn 88% and Cd 12% LB Film
Line is a fit to S = 5/2 Brillouin function
Using N = 5 x 10^17 spins
30
25
20
15
10
5
0
0
1
2
3
4
5

cadmium octadecylphosphonate bilayers act as nonfunctional spacers and increase the distance between adjacent manganese layers to 100Å in type I films and 150Å in type II films, Figure 5-1. In both types of film, a transition to long range order was observed at a temperature of 10.5 K, about 3 K lower than the ordering temperature of the pure manganese LB films. The difference in the ordering temperatures between the expanded manganese films and the pure manganese LB film is attributed to nonmagnetic impurities incorporated into the manganese layers in the alternating manganese/cadmium LB films. The impurities act to break up the domains of manganese spins and result in a decrease of the correlation length of the manganese domains within each manganese layer. A reduction of the ordering temperature is, therefore, expected.

Magnetic measurements were performed on additional LB samples containing manganese and cadmium ions combined in the inorganic portions of the films. One sample contained 34% Cd mixed into the manganese layers and another contained 12% Cd in the manganese layers. In both samples, the amount of nonmagnetic impurities was too large and magnetic exchange between the manganese moments was not observed. The magnetization data was fit using Curie laws. The results illustrate that the magnetic behavior of the LB films obey predictions set by basic theories of magnetism, but more importantly it demonstrates that inorganic properties observed in solid-state materials may be incorporated into Langmuir-Blodgett films.

REFERENCES

(1) de Jongh, L. J. In *Magnetic Properties of Layered Transition Metal Compounds*; L. J. de Jongh, Ed.; Kluwer Academic Publishers: Dordrecht, 1990; pp 1-51.

(2) *Solid State Chemistry: Compounds*; Cheetham, A. K.; Day, P., Ed.; Clarendon Press: Oxford, 1992.

(3) Day, P. *Chem. Br.* **1983**, 306-314.

(4) *Extended Linear Chain Compounds*; Miller, J. S., Ed.; Plenum Press: New York, 1983.

(5) Arts, A. F. M.; Wijn, H. W. D. In *Magnetic Properties of Layered Transition Metal Compounds*; L. J. D. Jongh, Ed.; Kluwer Academic Publishers: Dordrecht, 1990; pp 191-229.

(6) Witteveen, H. T. *Physica* **1974**, *71*, 204-236.

(7) Arend, H.; Huber, W.; Mischgofsky, F. H.; Leeuwen, G. K. R.-v. *Journal of Crystal Growth* **1978**, *43*, 213-223.

(8) Kind, R.; Plesko, S.; Arend, H.; Blinc, R.; Zeks, B.; Seliger, J.; Lozar, B.; Slak, J.; Levstik, A.; Filipic, C.; Zagar, V.; Lahajnar, G.; Milia, F.; Chapuis, G. *J. Chem. Phys.* **1979**, *71*, 2118-2130.

(9) Day, P. *Phil. Trans. R. Soc. Lond. A* **1985**, *314*, 145-158.

(10) Stead, M. J.; Day, P. *J. Chem. Soc. Dalton Trans.* **1982**, 1081-1084.

(11) de Jongh, L. J.; Miedema, A. R. *Adv. Phys.* **1974**, *24*, 1-260.

(12) Groenendijk, H. A.; Duyneveldt, A. J. v.; Willett, R. D. *Physica* **1980**, *101B*, 320 - 328.

(13) Cao, G.; Lynch, V. M.; Swinnea, J. S.; Mallouk, T. E. *Inorg. Chem.* **1990**, *29*, 2112-2117.

(14) Cao, G.; Lee, H.; Lynch, V. M.; Mallouk, T. E. *Solid State Ionics* **1988**, *26*, 63-69.

(15) Cao, G.; Lee, H.; Lynch, V. M.; Mallouk, T. E. *Inorg. Chem.* **1988**, *27*, 2781-2785.

(16) Cao, G.; Lynch, V. M.; Yacullo, L. N. *Chem. Mater.* **1993**, *5*, 1000-1006.

(17) Clearfield, A. *Comm. Inorg. Chem.* **1990**, *10*, 89-128.

(18) Martin, K. J.; Squattrito, P. J.; Clearfield, A. *Inorg. Chim. Acta* **1989**, *155*, 7-9.

(19) Cunningham, D.; Hennelly, P. J. D. *Inorg. Chim. Acta* **1979**, *37*, 95-102.

(20) Drumel, S.; Janvier, P.; Barboux, P.; Bujoli-Doeuff, M.; Bujoli, B. *Inorg. Chem.* **1995**, *34*, 148-156.

(21) Cao, G.; Hong, H.-G.; Mallouk, T. E. *Acc. Chem. Res.* **1992**, *25*, 420-427.

(22) Cao, G.; Mallouk, T. E. *Inorg. Chem.* **1991**, *30*, 1434-1438.

(23) Brousseau, L. C.; Aoki, K.; Yang, H. C.; Mallouk, T. E. In *Interfacial Design and Chemical Sensing*; T. E. Mallouk and D. J. Harrison, Ed.; American Chemical Society: Washington, D. C., 1994; Vol. ACS Symposium Series 561; pp 60-70.

(24) Kepley, L. J.; Sackett, D. D.; Bell, C. M.; Mallouk, T. E. *Thin Solid Films* **1992**, *208*, 132-136.

(25) Hong, H.-G.; Sackett, D. D.; Mallouk, T. E. *Chem. Mater.* **1991**, *3*, 521-527.

(26) Lee, H.; Kepley, L. J.; Hong, H.-G.; Mallouk, T. E. *J. Am. Chem. Soc.* **1988**, *110*, 618-620.

(27) Lee, H.; Kepley, L. J.; Hong, H.-G.; Akhter, S.; Mallouk, T. E. *J. Phys. Chem.* **1988**, *92*, 2597-2601.

(28) Putvinski, T. M.; Schilling, M. L.; Katz, H. E.; Chidsey, C. E. D.; Mujsce, A. M.; Emerson, A. B. *Langmuir* **1990**, *6*, 1567-1571.

(29) Vermeulen, L. A.; Snover, J. L.; Sapochak, L. S.; Thompson, M. E. *J. Am. Chem. Soc.* **1993**, *115*, 11767-11774.

(30) Zeppenfeld, A. C.; Fiddler, S. L.; Ham, W. K.; Klopfenstein, B. J.; Page, C. J. *J. Am. Chem. Soc.* **1994**, *116*, 9158-9165.

(31) Agarwal, V. K. *Physics Today* **1988**, 40.

(32) Zasadzinski, J. A.; Viswanathan, R.; Madsen, L.; Garnaes, J.; Schwartz, D. K. *Science* **1994**, *263*, 1726-1733.

(33) Ulman, A. *An Introduction to Ultrathin Organic Films: From Langmuir-Blodgett to Self-Assembly*; Academic Press: Boston, 1991.

(34) Pomerantz, M.; Dacol, F. H.; Segmüller, A. *Phys. Rev. Lett.* **1978**, *40*, 246-249.

(35) Viswanathan, R.; Zasadzinski, J. A.; Schwartz, D. K. *Science* **1993**, *261*, 449.

(36) Bain, C. D.; Troughton, E. B.; Tao, Y.-T.; Evall, J.; Whitesides, G. M.; Nuzzo, R. G. *J. Am. Chem. Soc.* **1989**, *111*, 321-335.

(37) Strong, L.; Whitesides, G. M. *Langmuir* **1988**, *4*, 546.

(38) Sagiv, J. *J. Am. Chem. Soc.* **1980**, *102*, 92.

(39) Maoz, R.; Sagiv, J. *J. Colloid Interface Sci.* **1984**, *100*, 465-496.

(40) Wasserman, S. R.; Tao, Y.-T.; Whitesides, G. M. *Langmuir* **1989**, *5*, 1074-1087.

(41) Langmuir, I. *J. Am. Chem. Soc.* **1917**, *39*, 1848-1906.

(42) Gaines, G. J. *Insoluble Monolayers at Liquid-Gas Interfaces*; Wiley-Interscience: New York, 1966.

(43) Blodgett, K. A.; Langmuir, I. *Phys. Rev.* **1937**, *51*, 964.

(44) Blodgett, K. B. *J. Am. Chem. Soc.* **1935**, *57*, 1007.

(45) Schwartz, D. K.; Garnaes, J.; Viswanathan, R.; Zasadzinski, J. A. N. *Science* **1992**, *257*, 508-511.

(46) Viswanathan, R.; Schwartz, D. K.; Garnaes, J.; Zasadzinski, J. A. N. *Langmuir* **1992**, *8*, 1603-1607.

(47) Prakash, M.; Ketterson, J. B.; Dutta, P. *Thin Solid Films* **1985**, *134*, 1-4.

(48) Prakash, M.; Dutta, P.; Ketterson, J. B.; Abraham, B. M. *Chem. Phys. Lett.* **1984**, *111*, 395.

(49) Lesslauer, W.; Blasie, J. K. *Biophysical Journal* **1972**, *12*, 175.

(50) Schwartz, D. K.; Viswanathan, R.; Zasadzinski, J. A. N. *Langmuir* **1993**, *9*, 1384-1391.

(51) Bloch, F. *Z. Phys.* **1930**, *61*, 206.

(52) Onsager, L. *Phys. Rev.* **1944**, *65*, 117-149.

(53) Mermin, N. D.; Wagner, H. *Phys. Rev. Lett.* **1966**, *17*, 1133-1136.

(54) Hirakawa, K.; Ikeda, H. In *Magnetic Properties of Layered Transition Metal Compounds*; L. J. d. Jongh, Ed.; Kluwer Academic Publishers: Dordrecht, 1990; pp 231-270.

(55) Endoh, Y.; Yamada, K.; Birgeneau, R. J.; Gabbe, D. R.; Jenssen, H. P.; Kastner, M. A.; Peters, C. J.; Picone, P. J.; Thurston, T. R.; Tranquada, J. M.; Shirane, G.; Hidaka, Y.; Oda, M.; Enomoto, Y.; Suzuki, M.; Murakami, T. *Phys. Rev. B* **1988**, *37*, 7443-7453.

(56) Birgeneau, R. J.; Skalyo, J.; Shirane, G. *Phys. Rev. B* **1971**, *3*, 1736-1749.

(57) Carling, S. G.; Day, P.; Visser, D.; Kremer, R. K. *J. Solid State Chem.* **1993**, *106*, 111-119.

(58) Carling, S. G.; Day, P.; Visser, D. *J. Phys.: Condens. Matter.* **1995**, *7*, L109-L113.

(59) Pomerantz, M.; Pollak, R. A. *Chem. Phys. Lett.* **1975**, *31*, 602-604.

(60) Pomerantz, M. In *In NATO ASI Series - Phase Transitions in Surface Films*; J. G. Dash and J. Ruvalds, Ed.; Plenum: New York, 1980; pp 317-346.

(61) Bringley, J. F.; Averill, B. A. *Chem. Mater.* **1990**, *2*, 180-186.

(62) Kanatzidis, M. C.; Wu, C.-G.; Marcy, H. O.; Kannewurf, C. R. *J. Am. Chem. Soc.* **1989**, *111*, 4139-4141.

(63) Day, P.; Ledsham, R. D. *Mol. Cryst. Liq. Cryst.* **1982**, *86*, 163-174.

(64) Thompson, M. E. *Chem. Mater.* **1994**, *6*, 1168-1175.

(65) Ozin, G. A. *Adv. Mater.* **1992**, *4*, 612-649.

(66) *Supramolecular Architecture. Synthetic Control in Thin Films and Solids*.; Bein, T., Ed.; American Chemical Society: Washington DC, 1992; Vol. 499, pp 441.

(67) Beck, J. S.; Vartuli, J. C.; Roth, W. J.; Leonowicz, M. E.; Kresge, C. T.; Schmitt, K. D.; Chu, C. T.-W.; Olson, D. H.; Sheppard, E. W.; McCullen, S. B.; Higgins, J. B.; Schlenker, J. L. *J. Am. Chem. Soc.* **1992**, *114*, 10834-10843.

(68) Monnier, A.; Schuth, F.; Huo, Q.; Kumar, D.; Margolese, D.; Maxwell, R. S.; Stucky, G. D.; Krishnamurty, M.; Petroff, P.; Firouzi, A.; Janicke, M.; Chmelka, B. F. *Science* **1993**, *261*, 1299-1303.

(69) Kresge, C. T.; Leonowicz, M. E.; Roth, W. J.; Vartuli, J. C.; Beck, J. S. *Nature* **1992**, *359*, 710-713.

(70) Matijevic, E. *Chem. Mater.* **1993**, *5*, 412-426.

(71) Scoberg, D. J.; Grieser, F.; Furlong, D. N. *J. Chem. Soc., Chem. Commun.* **1991**, *7*, 515-517.

(72) *Langmuir-Blodgett Films*; Roberts, G. G., Ed.; Plenum Press: New York, 1990.

(73) Schwartz, D. K.; Viswanathan, R.; Garnaes, J.; Zasadzinski, J. A. *J. Am. Chem. Soc.* **1993**, *115*, 7374-7380.

(74) Shih, M. C.; Peng, J. B.; Huang, K. C.; Dutta, P. *Langmuir* **1993**, *9*, 776-778.

(75) Outka, D. A.; Stöhr, J.; Rabe, J. P.; Swalen, J. D.; Rotermund, H. H. *Phys. Rev. Lett.* **1987**, *59*, 1321-1324.

(76) Byrd, H.; Pike, J. K.; Talham, D. R. *J. Am. Chem. Soc.* **1994**, *116*, 7903-7904.

(77) Byrd, H.; Pike, J. K.; Talham, D. R. *Chem. Mater.* **1993**, *5*, 709-715.

(78) Kuhn, H.; Möbius, D.; Bücher, H. In *Physical Methods of Chemistry*; A. Weissberger and B. Rossiter, Ed.; John Wiley and Sons: 1972; Vol. 1, Part IIIB; pp 577-715.

(79) Seip, C. T.; Byrd, H.; Talham, D. R. *Inorg. Chem.* **1996**, *35*, 3479-3483.

(80) Prien, E. L.; Prien, E. L. *American Journal of Medicine* **1968**, *45*, 654.

(81) Alberti, G.; Casciola, M.; Costantino, U.; Vivani, R. *Adv. Mater.* **1996**, *8*, 291-303.

(82) Kern, W. *J. Electrochem. Soc.* **1990**, *137*, 1887-1892.

(83) Netzer, L.; Sagiv, J. *J. Am. Chem. Soc.* **1983**, *105*, 674-676.

(84) Wagner, C. D.; Davis, L. E.; Zeller, M. V.; Taylor, J. A.; Raymond, R. M.; Gale, L. H. *Surf. Interface Anal.* **1981**, *3*, 211.

(85) *5000 Series ESCA Systems Version 2.0 Instruction Manual*; Perkin-Elmer Physical Electronics Division: Eden Prairie, MN, 1989.

(86) Brundle, C. R.; Hopster, H.; Swalen, J. D. *J. Chem. Phys.* **1979**, *70*, 5190-5196.

(87) *Practical Surface Analysis*; 2nd ed.; Briggs, D.; Seah, M. P., Ed.; John Wiley and Sons: Chichester, 1990; Vol. 1.

(88) Pike, J. K.; Byrd, H.; Morrone, A. A.; Talham, D. R. *Chem. Mater.* **1994**, *6*, 1757-1765.

(89) Seah, M. P.; Dench, W. A. *Surf. Interface Anal.* **1979**, *1*, 1-11.

(90) Allara, D. L.; Nuzzo, R. G. *Langmuir* **1985**, *1*, 45.

(91) Porter, M. D.; Bright, T. B.; Allara, D. L.; Chidsey, C. E. D. *J. Am. Chem. Soc.* **1987**, *109*, 3559-3568.

(92) Wood, K. A.; Snyder, R. G.; Strauss, H. L. *J. Chem. Phys.* **1989**, *91*, 5255-5267.

(93) Byrd, H.; Whipps, S.; Pike, J. K.; Talham, D. R. *Thin Solid Films* **1994**, *244*, 768-771.

(94) Nakamoto, K. *Infrared and Raman Spectra of Inorganic and Coordination Compounds;* 3rd ed.; John Wiley & Sons: New York, 1978.

(95) Susi, H.; Smith, A. M. *Journal of the American Oil Chemists' Society* **1960**, *37*, 431-435.

(96) Bellamy, L. J. *The Infra-red Spectra of Complex Molecules;* 3rd ed.; Chapman and Hall: London, 1975.

(97) Hayaki, J. *J. Chem. Phys.* **1975**, *63*, 1732.

(98) Thomas, L. C.; Chittenden, R. A. *Spectrochim. Acta* **1970**, *26A*, 781-800.

(99) Haller, G. L.; Rice, R. W. *J. Phys. Chem.* **1970**, *74*, 4386-4393.

(100) Tillman, N.; Ulman, A.; Schildkraut, J. S.; Penner, T. L. *J. Am. Chem. Soc.* **1988**, *110*, 6136-6144.

(101) Frey, B. L.; Hanken, D. G.; Corn, R. M. *Langmuir* **1993**, *9*, 1815-1820.

(102) Mitsuya, M.; Taniguchi, Y.; Akagi, M. *J. Colloid and Interface Sci.* **1983**, *92*, 291.

(103) Miki, T.; Inaoka, K.; Sato, K.; Okada, M. *Japan. J. Appl. Phys.* **1985**, *24*, L672.

(104) Agarwal, V.; Igasaki, Y.; Mitsuhashi, J. *Japan. J. Appl. Phys.* **1976**, *15*, 2327.

(105) Wang, R.-C.; Zhang, Y.; Hu, H.; Frausto, R. R.; Clearfield, A. *Chem. Mater.* **1992**, *4*, 864-870.

(106) Zhang, Y.; Clearfield, A. *Inorg. Chem.* **1992**, *31*, 2821-2826.

(107) Le Bideau, J.; Jouanneaux, A.; Payen, C.; Bujoli, B. *J. Mater. Chem.* **1994**, *4*, 1319-1323.

(108) Alberti, G.; Costantino, U.; Allulli, S.; Tomassini, N. *J. Inorg. Nucl. Chem.* **1978**, *40*, 1113-1117.

(109) Scott, K. J.; Zhang, Y.; Wang, R.; Clearfield, A. *Chem. Mater.* **1995**, *7*, 1095-1102.

(110) Katz, H. E.; Schilling, M. L.; Chidsey, C. E. D.; Putvinski, T. M.; Hutton, R. S. *Chem. Mater.* **1991**, *3*, 699-703.

(111) Katz, H. E.; Scheller, G.; Putvinski, T. M.; Schilling, M. L.; Wilson, W. L.; Chidsey, C. E. D. *Science* **1991**, *254*, 1485-1487.

(112) Yang, H. C.; Aoki, K.; Hong, H.; Sackett, D. D.; Arendt, M. F.; Yau, S.; Bell, C. M.; Mallouk, T. E. *J. Am. Chem. Soc.* **1993**, *115*, 11855-11862.

(113) Byrd, H.; Whipps, S.; Pike, J. K.; Ma, J.; Nagler, S. E.; Talham, D. R. *J. Am. Chem. Soc.* **1994**, *116*, 295-301.

(114) Byrd, H.; Pike, J. K.; Showalter, M. L.; Whipps, S.; Talham, D. R. In *Interfacial Design and Chemical Sensing*; T. E. Mallouk and D. J. Harrison, Ed.; American Chemical Society: Washington, 1994; Vol. ACS Symposium Series 561; pp 49-59.

(115) Le Bideau, J.; Payen, C.; Bujoli, B.; Palvadeau, P.; Rouxel, J. *J. Magn. Magn. Mater.* **1995**, *140-144*, 1719-1720.

(116) Gatteschi, D.; Sessoli, R. *Magnetic Resonance Review* **1990**, *15*, 1-45.

(117) Yamada, I.; Morishita, I.; Tokuyama, T. *Physica* **1983**, *115B*, 179-189.

(118) Benner, H.; Boucher, J. P. In *Magnetic Properties of Layered Transition Metal Compounds*; L. J. de Jongh, Ed.; Kluwer Academic: Dordrecht, 1990; pp 323-378.

(119) Patyal, B. R.; Willett, R. D. *Magnetic Resonance Review* **1990**, *15*, 47-82.

(120) Richards, P. M.; Salamon, M. B. *Phys. Rev. B* **1974**, *9*, 32-45.

(121) Lines, M. E. *J. Phys. Chem. Solids* **1970**, *31*, 101-116.

(122) Rushbrooke, G. S.; Wood, P. J. *Molec. Phys.* **1958**, *1*, 257.

(123) Navarro, R. In *Magnetic Properties of Layered Transition Metal Compounds*; L. J. d. Jongh, Ed.; Kluwer Academic Publishers: Dordrecht, 1990; pp 105-190.

(124) Pokrovsky, V. L.; Uimin, G. V. In *Magnetic Properties of Layered Transition Metal Compounds*; L. J. de Jongh, Ed.; Kluwer Academic: Dordrecht, 1990; pp 53-103.

(125) Ferrieu, F.; Pomerantz, M. *Solid State Commun.* **1981**, *39*, 707-710.

(126) Pomerantz, M. *Surf. Sci.* **1984**, *142*, 556-570.

(127) Pomerantz, M. *Solid State Comm.* **1978**, *27*, 1413-1416.

(128) Mann, S.; Archibald, D. D.; Didymus, J. M.; Douglas, T.; Heywood, B. R.; Meldrum, F. C.; Reeves, N. J. *Science* **1993**, *261*, 1286-1292.

(129) Bryce, M. R.; Petty, M. C. *Nature* **1995**, *374*, 771-776.

(130) Cresswell, L. P.; Petty, M. C.; Wang, C. H.; Wherrett, B. S.; Ali-Adib, Z.; Hodge, P.; Ryan, T. G.; Allen, S. *Optics Comm.* **1995**, *115*, 271-275.

(131) Penner, T. L.; Motschmann, H. R.; Armstrong, N. J.; Ezenyilimba, M. C.; Williams, D. J. *Nature* **1994**, *367*, 49-51.

(132) Carlin, R. L. *Magnetochemistry;* 1st ed.; Springer-Verlag: Berlin, 1986.

(133) Laibinis, P. E.; Whitesides, G. M.; Allara, D. L.; Tao, Y.-T.; Parikh, A. N.; Nuzzo, R. G. *J. Am. Chem. Soc.* **1991**, *113*, 7152-7167.

(134) Bonosi, F.; Gabrielli, G.; Martini, G.; Ottaviani, M. F. *Langmuir* **1989**, *5*, 1037-1043.

(135) Ikegami, K.; Kuroda, S.-I.; Sugi, M.; Nakamura, T.; Tachibana, H.; Matsumoto, M.; Kawabata, Y. *J. Phys. Soc. Jpn.* **1992**, *61*, 3752-3765.

(136) Petford-Long, A. K. *Thin Solid Films* **1996**, *275*, 35 - 39.

(137) Labat, S.; Pichaud, B.; Thomas, O.; Alfonso, C.; Charai, A.; Barrallier, L.; Gilles, B.; Marty, A. *Thin Solid Films* **1996**, *275*, 29 - 34.

(138) Boeck, J. D.; Bruynseraede, C.; Bender, H.; Esch, A. V.; Roy, W.; Borghs, G. *Journal of Crystal Growth* **1995**, *150*, 1139-1143.

(139) Nebesny, K. W.; Collins, G. E.; Lee, P. A.; Chau, L.-K.; Danziger, J.; Osburn, E.; Armstrong, N. R. *Chem. Mater.* **1991**, *3*, 829-838.

(140) Breed, D. J.; Gilijamse, K.; Sterkenburg, J. W. E.; Miedema, A. R. *J. Appl. Phys.* **1970**, *41*, 1267.

(141) Breed, D. J.; Gilijamse, K.; Sterkenburg, J. W. E.; Miedema, A. R. *Physica* **1973**, *68*, 303-314.

(142) Subbaraman, K.; Zaspel, C. E.; Drumheller, J. E. *J. Appl. Phys.* **1996**, *79*, 5368 - 5370.

BIOGRAPHICAL SKETCH

Candace Tricia Seip was born in Regina, Saskatchewan, Canada, on July 13, 1971.

In the fall of 1989, Candace enrolled at the University of Regina, and, 4 years later, received her Bachelor of Science honours degree in Chemistry. After graduation, she moved to Gainesville, Florida, to attend graduate school.

Candace entered graduate school at the University of Florida in the fall of 1993, and by October of that year joined Dr. Daniel R. Talham's research group. After 4 years under Dan Talham's supervision, she defended her dissertation and graduated from the University of Florida with a Ph.D. in chemistry.

I certify that I have read this study and that in my opinion it conforms to acceptable standards of scholarly presentation and is fully adequate, in scope and quality, as a dissertation for the degree of Doctor of Philosophy.

Daniel R. Talham, Chairman
Associate Professor of Chemistry

I certify that I have read this study and that in my opinion it conforms to acceptable standards of scholarly presentation and is fully adequate, in scope and quality, as a dissertation for the degree of Doctor of Philosophy.

Russell S. Drago
Graduate Research Professor of Chemistry

I certify that I have read this study and that in my opinion it conforms to acceptable standards of scholarly presentation and is fully adequate, in scope and quality, as a dissertation for the degree of Doctor of Philosophy.

David E. Richardson
Professor of Chemistry

I certify that I have read this study and that in my opinion it conforms to acceptable standards of scholarly presentation and is fully adequate, in scope and quality, as a dissertation for the degree of Doctor of Philosophy.

John R. Reynolds
Professor of Chemistry

I certify that I have read this study and that in my opinion it conforms to acceptable standards of scholarly presentation and is fully adequate, in scope and quality, as a dissertation for the degree of Doctor of Philosophy.

Elizabeth Seiberling
Associate Professor of Physics

This dissertation was submitted to the Graduate Faculty of the Department of Chemistry in the College of Liberal Arts and Sciences and to the Graduate School and was accepted as partial fulfillment of the requirements for the degree of Doctor of Philosophy.

May, 1997

Dean, Graduate School